ENERGETICS OF LATE CHEMICAL REACTIONS IN NONIDEAL UNDERWATER DETONATIONS: PHASE I, PRELIMINARY THEORETICAL MODEL DEVELOPMENT

Michael Cowperthwaite
D. John Pastine
Julius W. Enig

ENIG ASSOCIATES, INC.

1995

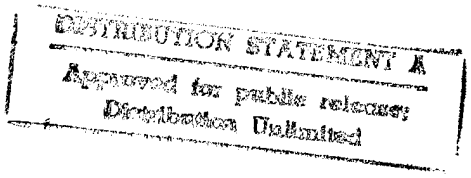

ONR
Office of Naval Research

ENERGETICS OF LATE CHEMICAL REACTIONS IN NONIDEAL UNDERWATER DETONATIONS: PHASE I, PRELIMINARY THEORETICAL MODEL DEVELOPMENT

Michael Cowperthwaite
D. John Pastine
Julius W. Enig

ENIG ASSOCIATES, INC.

1995

ONR
Office of Naval Research

ENERGETICS OF LATE CHEMICAL REACTIONS IN NONIDEAL UNDERWATER DETONATIONS: PHASE I, PRELIMINARY THEORETICAL MODEL DEVELOPMENT

Prepared by

Michael Cowperthwaite
D. John Pastine
Julius W. Enig

ENIG ASSOCIATES, INC.
11120 NEW HAMPSHIRE AVENUE, SUITE 500
SILVER SPRING, MARYLAND 20904-2633

October 1995

Contract No. N00014-95-C-0154

Prepared for

ONR
Office of Naval Research
Attn: Judah Goldwasser (ONR 333)
800 N. Quincy Street
Arlington, VA 22217-5660

Table of Contents

1. INTRODUCTION

1.1. General

This Final Report describes the complete research work that has been carried out starting 1 April 1995, under Office of Naval Research SBIR Phase I contract no. N00014-95-C-0154, in the area of energetics of late chemical reactions of metals in nonideal underwater detonations.

1.2. Background

The reaction of metallic fuels with the detonation products in all explosives is poorly understood to this day, but there is much evidence, albeit indirect, that the exothermic reaction that consumes aluminum takes place over a much longer time scale than that which consumes, say, TNT, RDX, or HMX. The probability of this late time reaction is greater in underwater explosions because the inertial confinement of the explosive products by the vast mass of surrounding water is much greater than any confinement by metal cases of explosions in air. Metallic fuels, principally aluminum, have been added to underwater explosives, and the aluminum oxidation is greatly affected by the confinement. It is well known that the "bubble energy" -- a uniquely underwater effect -- increases, relative to the nonaluminized material, as the aluminum/oxygen ratio increases from 0 to 1. The "shock wave energy" reaches a maximum for an Al/O ratio of about 0.4 in some TNT/RDX mixtures. The aluminum content is used to fine tune the bubble and shock energies -- which are related to underwater target damage -- depending on the target.

Metallized composite explosives provide the means of tailoring the chemical energy release rate in the detonation process because the metal additive is capable of reacting with the explosive's products to support both the propagation of the detonation wave and the unsteady flow in the release wave behind the detonation front. Because of this role of the metal in the detonation process, metallized explosives are said to be nonideal explosives; a consequence is that there are not predictive models for quantifying their behavior. In addition, because the amount of metal reacting to support the detonation is not known, and thermo-hydrodynamic codes for calculating Chapman-Jouguet (CJ) parameters for CHNO explosives cannot be used to predict detonation parameters in metallized explosives, the detonation process is also said to be nonideal. Consequently, the capability to tailor the energy release in metallized explosives for underwater applications depends on our ability to control the reactions of the metal in the nonideal detonation process.

Metallized explosives are examples of composite explosives that are nonideal explosives, i.e, where mass transport between oxidizer and fuel is an important rate-determining process, unlike ideal explosives, which are molecular mixtures of fuel and oxidizer that are separated by extremely short distances, i.e., bond lengths. Because reaction rates in ideal explosives are so fast, explosive performance can be modeled as depending only on equilibrium states along the Chapman-Jouguet (CJ) isentrope behind the CJ plane, upstream of which all explosive is reacted. The modeling of nonideal detonations, i.e., detonations of nonideal explosives, is much more complicated, depending on the heterogeneity of the fuel/oxidizer mixture, diffusion rates, mixing distances, reaction times, and energy release rates, none of which are explicitly needed to describe ideal detonations.

Ideal and nonideal explosives differ greatly in their failure diameter: failure diameters in the former are generally of the order of millimeters; those of the latter are in the centimeter range because of the heterogeneity and slow reaction rates of the composite explosives.

The energy release processes in composites, while relatively slow, are far more complex than in ideal explosives. As a consequence, it is a difficult problem to couple these "microscopic" rate-determining processes to the "macroscopic" compressible fluid dynamics of the complex detonation products and the "early" compressible and "later" incompressible flows in the water.

For ideal and nonideal detonation processes, the flows in the steady-state reaction zones satisfy the Rankine-Hugoniot (RH) jump conditions and become sonic at the CJ point where the energy release rate becomes zero.[1,2] But whereas all the available chemical energy is used to support the steady-state flow in the ideal detonation, it is not used in the nonideal detonation because the time scale for the decomposition of the explosive is significantly different from the time scales of the reactions of the metal with the detonation products. The detonation parameters in the nonideal detonation thus can be tailored by controlling the amount of metal that reacts in the steady-state reaction zone.

For both detonation processes, the flows in the unsteady release waves behind the CJ planes are governed by the differential equations expressing the conservation of mass, momentum, and energy for inviscid, adiabatic flow. The release wave in the ideal detonation process is isentropic and is, thus, represented in the specific volume-pressure v-p plane by the isentrope of the detonation products passing through the CJ point. Because of metal reactions, however, the release wave in the nonideal detonation process is not isentropic and is, thus, represented in the v-p plane by a reactive release adiabat passing through the CJ point. Moreover, the entropy increases with volume along such a reactive adiabat because entropy is produced by the reactions of the metal with the products of the explosive. Thus, the energy release rate for underwater applications can be tailored by controlling the reactions of the metal with the explosive's products in the release wave.

Because the areas under the CJ isentrope and CJ release adiabat in the v-p plane are directly related to the amounts of available chemical energy in the explosive compositions, the energy release rate in the release wave can be tailored by controlling the pressure when the metal begins to react as well as its subsequent rate of reaction. In other words, the shapes of the reactive release adiabats can only be changed by varying both the onset and subsequent rates of the metal reactions in the release wave.

It follows from the discussion of the detonation process that ideal detonations can be adequately described by thermodynamic processes, but nonideal detonation cannot because the energy release rate is governed by kinetic processes with different time scales. Semi-empirical thermo-hydrodynamic studies of nonideal explosives, of the type performed by Mader[3] and Cowperthwaite,[4] provide phenomenological information about the energy release rate, but do not provide the information and knowledge required to control it. Thus, a more basic approach must be taken to provide a means of controlling the energy release rate in metallized explosives. In such an approach, we must first identify the most important kinetic processes governing the energy release rate and then develop realistic models for them, containing parameters related to

the physical and chemical properties of the explosive compositions.

1.3. Dividing Up the Kinds of Explosives

Explosives are generally divided into two classes, ideal and nonideal.[5] We have noted that ideal explosives may be defined as those in which fuel and oxidizer are homogeneously mixed at the molecular level. That is to say, the irreducible fuel element and the irreducible oxidizer element are either, within the same molecule in a grain or crystal of identical molecules, or, are at least nearest neighbors in separate molecules in a bimolecular crystal or grain. Ideal explosives are characterized by short reaction zones and exhibit little or no delayed reaction. Nonideal explosives are a broader class usually composed of grains of ideal explosive homogeneously mixed with other grains of fuel and/or oxidizer. They may behave more or less like ideal explosives depending on whether they contain more or less ideal explosive constituents. They are composite explosives, exhibit longer reaction zones, and in general considerably more "delayed" reaction.

For the purpose of modeling nonideal explosives, we divide these into two categories: the *first* category, which we call *totally nonideal* explosives comprises explosives in which the fuel and oxidizer each appear only in separate grains. Examples are AP/wax and AP/Al, *without* any energetic binder. It must be emphasized that such mixtures are not practical for service use, but they have been tried out as experimental mixtures and their detonation velocities and sensitivities have been measured by D. Price, et al. [6,7] (The AP/Al mixture fell in Price's Category 2 classification.) Their utility is that they are excellent examples of mixtures for which the gross heterogeneity, diffusion rates, mixing distances, etc. can be modeled unencumbered by any rapid reaction of an explosive molecule containing both fuel and oxidizer. It is this category of nonideal explosives that has been emphasized in this Phase I theoretical effort, which is described below in Sections 2 and 3.

The *second* category, which we call somewhat ambiguously *nonideal* explosives, are a mixture of an ideal explosive and at least one separate fuel or oxidizer, e.g., PBXN-102 (HMX/Al/binder) and PBXW-115(Q) (RDX/AP/Al/binder). Thus, this category can be viewed as an admixture of ideal and totally nonideal explosives. Most practical explosives fall within this category, particularly those used by the Navy. Model development for this category of nonideal explosive is left for a future Phase II effort.

The field of nonideal explosives has been extensively investigated for many years, particularly by the underwater explosives community. As early as 1918, German studies showed that the addition of 15-20% aluminum increases underwater performance. There exists a large number of Navy-developed plastic bonded explosives containing ammonium perchlorate and/or aluminum: PBXC-117(Q), PBXN-102, PBXN-103, PBXN-105, PBXN-109, PBXW-107(Q), PBXW-114(Q), PBXW-115(Q), all of which are cast; PBXN-4, PBXN-7 (Type I), all of which are pressed; PBXN-201, which is extrudable and injection moldable.

E. Anderson provides an excellent review of explosives, and in particular the effects of explosive composition ingredients, charge diameter, failure diameter, and confinement on performance of nonideal explosives. The Detonation Symposia provide an extensive literature on nonideal detonations, including some of the important results from the Lawrence Livermore

National Laboratory.

Recently, some very interesting small-scale laboratory tests by P. Miller and R. Guirguis were performed comparing product gas expansion rates against a column of water for ideal and nonideal aluminized explosives. JWL equation of state incorporating a time-dependent late energy release was adjusted to reproduce the experimental nonideal explosive results. These authors also calculated the effects of late chemical reactions on the bubble oscillation and pressure pulse induced in water by nonideal explosives. Their energy release was governed by the rate law $d\lambda/dt=a(1-\lambda)^{1/2}p^{1/6}$, where λ, p, t, and a are, respectively, the progress variable, pressure, time, and a constant.

1.4. Current Modeling Effort

This report describes a preliminary model of kinetic and thermo-hydrodynamic processes that define the nonideal detonation of a *totally nonideal* explosive: an AP/Al mixture.

Section 2 presents a thermo-hydrodynamic description of reactive explosive compositions containing aluminum and, in particular, a description of the nonideal detonation process in ammonium perchlorate/aluminum and CHNO explosive/Al compositions. The specific energy relationships for these reacting compositions are presented in which Mie-Gruneisen equations of state are derived, including the temperature, and used for the solid components. Also the equations of steady state detonation in AP/Al compositions are presented.

In Section 3 we present a theory describing the kinetic processes by which $Al/Al_2O_3/AP$ products react. Key here is the application of the phenomenon of anomalously high ionic conduction, which are exhibited by the β-aluminas, through "tunnels" through which cations can move freely. This provides a plausible explanation of events in Al/explosive reactions. Statistical mechanical concepts are employed to provide reaction rate equations for Al and AP.

The theoretical results of Sections 2 and 3 provides a preliminary physical model based on first principles, which will be integrated into a compressible flow code in the next phase of this work, which is to improve, extend, and validate the model.

1.5. Acknowledgement

This report is based upon work supported by the Office of Naval Research under Small Business Innovative Research (SBIR) Program Phase I contract no. N00014-95-C-0154.

We wish to thank Drs. Phil Miller and Raafat Guirguis of the Naval Surface Warfare Center Indian Head Division, White Oak for providing profitable discussions and information on their experimental and theoretical work on nonideal detonations of aluminized explosives, Dr. Jagadish Sharma, also of the NSWCIHD, White Oak, for fruitful discussions on the crystallography of ammonium perchlorate, Erwin Anderson of NSWCIHD, White Oak, for informative discussions on nonideal explosives, and to Dr. William Davis, formerly of the Los Alamos National Laboratory, for steering us to the work of E. O'Connor.

2. THERMO-HYDRODYNAMICS OF REACTING EXPLOSIVE MIXTURES CONTAINING ALUMINUM (Al)

In this section of the report, we formulate a global thermodynamic description of reacting explosive compositions containing Al. Such a description is required in order to perform analytical and numerical studies of the role played by Al in the nonideal detonation process in ammonium perchlorate (AP)/Al compositions as well as CHNO explosive/Al compositions.

In Sections 2.1 and 2.2, we construct the specific energy e relationships for reacting AP/Al and CHNO/Al compositions with their solid components governed by generalized Mie-Gruneisen (MG) equations of state. These constructions must be based on the mass balance equations for the decomposing explosive and the Al reactions because the Al combines with oxygen-containing products of the explosive to form aluminum oxide Al_2O_3. We also derive the mass balance equations for Al spheres reacting with oxygen to form an outer coating of Al_2O_3.

In Section 2.3, we presented the particular MG EOS that were constructed for AP, Al, and Al_2O_3, and the EOS used for the explosive's products.

In Section 2.4, we consider steady-state (SS) detonation waves, and the relationship between the SS reaction zone length and reaction time in AP. We also develop a prototype model for SS, nonideal detonation in a CHNO/Al composition to provide a better understanding of the nonideal detonation process in explosive compositions containing Al, and demonstrate why global kinetic expressions must be constructed for the Al reactions. A procedure for constructing such a global kinetic expression will be presented in the next Section 3 of this report.

2.1. A Specific Energy Relationship for a Reacting AP/Al Mixture

Because of the complex nature of reactive explosive mixtures in the 10-400 kbar region treatments of detonation phenomena must be based on assumptions regarding the significant chemical and physical processes. Here, our formulation of an e-relationship for AP/Al mixtures with compressible, condensed components is based on the following assumptions:

A.1. The AP decomposes to form a mixture of products with a fixed composition containing oxygen (O_2), nitrogen (N_2), water (H_2O), and chlorine (Cl_2).

A.2. The AP produces enough O_2 to react with all the Al in the AP/Al mixture.

A.3. The Al_2O_3 produced by the reaction of Al and O_2 can be either solid α-Al_2O_3 or γ-Al_2O_3 , depending on the thermodynamic state.

A.4. Each constituent in the reacting AP/Al mixture has the same pressure p and is governed by its own equation of state (EOS) relating e, p, and specific volume v.

It follows from A.1 and A.3 that our relation for e must contain two reaction coordinates, say λ_1 and λ_2, to account, respectively, for the decomposition of the AP and the reaction of Al and O_2 to form solid Al_2O_3. In addition, we must account for the formation of either α-Al_2O_3 or

γ-Al_2O_3 and formulate a condition to determine when one is formed and not the other. Such a condition will be formulated later when we consider the EOS of Al_2O_3. At this stage, it should also be noted that we will not consider melting of either the Al or the solid Al_2O_3.

When mixture rules for the total internal energy E_m and volume V_m of such an AP/Al composition are specified, these assumptions allow us to formulate an e-relationship for this composition in terms of p, the specific volumes of its components, and the reaction coordinates λ_1 and λ_2. Our formulation of such an e-relationship, here, will be carried out in two steps. In the first step, we will define the reaction coordinates λ_1 and λ_2 and derive equations for the masses of the components in our reacting AP/Al mixture in terms of λ_1 and λ_2. In the second step, we will use the mixture rules for E_m and V_m, and the e=e(p,v) EOS of the components to derive our equation for e.

2.1.1. Mass Balance Equations for an AP/Al Composition

We consider an AP/Al composition with an initial mass M_0, an initial mass fraction of AP, $\alpha^0_{AP} = m^0_{AP}/M_0$, and an initial mass fraction of Al, $\alpha^0_{Al} = m^0_{Al}/M_0$, and also recall that it is customary for such a mixture to set M_0=100g. To write the mass balance equations for such a mixture subject to A.1 and A.3, we must consider the following chemical reactions:

$$NH_4 Cl O_4 = O_2 + 2H_2O + \tfrac{1}{2}N_2 + \tfrac{1}{2}Cl_2 \qquad \text{(R.1)}$$

$$2Al + 3/2\ O_2 = (Al_2O_3)^i_s,\ i=1 \text{ or } 2 \qquad \text{(R.2)}$$

with i=1 and i=2 used, respectively, to denote α-Al_2O_3 and γ-Al_2O_3. We first let M_i denote the molecular weight of a species S_i, and see from (R.1) and R.2) that $m^0_{AP}/M_{AP} \geq 3m^0_{Al}/4M_{Al}$ is the condition for our composition to satisfy A.2. We next let m_i denote the mass of a species S_i and write the law of definite proportions for (R.1) and (R.2) with extents of reaction ξ_1 and ξ_2 as

$$-\frac{dm_{AP}}{M_{AP}} = \frac{dm^1_{O_2}}{M_{O_2}} = \frac{dm_{H_2O}}{2M_{H_2O}} = \frac{dm_{Cl_2}}{\tfrac{1}{2}M_{Cl_2}} = \frac{dm_{N_2}}{\tfrac{1}{2}M_{N_2}} = d\xi_1 \qquad (2.1.1)$$

$$-\frac{dm_{Al}}{2M_{Al}} = -\frac{dm^2_{O_2}}{\frac{3}{2}M_{O_2}} = \frac{dm^i_{Al_2O_3}}{M_{Al_2O_3}} = d\xi_2 \qquad (2.1.2)$$

with

$$dm_{O_2} = dm^1_{O_2} + dm^2_{O_2} \qquad (2.1.3)$$

Here the superscripts 1 and 2 refer to the respective equations, R.1 and R.2.

Formally integrating these equations and introducing the reaction coordinates

$$\lambda_1 = \xi_1 \frac{M_{AP}}{m^0_{AP}} \text{ and } \lambda_2 = \xi_2 \frac{2M_{Al}}{m^0_{Al}},$$

and the mass fractions

$$\frac{2M_{H_2O}}{M_{AP}} = \alpha_1 , \frac{M_{O_2}}{M_{AP}} = \alpha_2 , \frac{M_{N_2}}{2M_{AP}} = \alpha_3 , \frac{M_{Cl_2}}{2M_{AP}} = \alpha_4 , \frac{2M_{Al}}{M_{Al_2O_3}} = \beta_1 , \frac{3M_{O_2}}{2M_{Al_2O_3}} = \beta_2$$

gives the equations for the masses of the species in our reactive AP/Al mixture as

$$m_{AP} = m_{AP}^0(1-\lambda_1) \qquad (2.1.4)$$

$$m_{H_2O} = m_{AP}^0\alpha_1\lambda_1 \qquad (2.1.5)$$

$$m_{N_2} = m_{AP}^0\alpha_3\lambda_1 \qquad (2.1.6)$$

$$m_{Cl_2} = m_{AP}^0\alpha_4\lambda_1 \qquad (2.1.7)$$

$$m_{O_2} = m_{AP}^0\lambda_1 - m_{Al}^0\,\beta_2\lambda_2/\beta_1 \qquad (2.1.8)$$

$$m_{Al} = m_{Al}^0(1-\lambda_2) \qquad (2.1.9)$$

$$m_{Al_2O_3}^i = (m_{Al}^0/\beta_1)(\lambda_2-\lambda_3) \qquad (2.1.10)$$

with $m_{Al_2O_3}^i$ used to denote the mass of $(Al_2O_3)_s$. It follows from these equations that the masses of the condensed components are defined by Eqs. (2.1.4), (2.1.9), and (2.1.10) and that the mass of the fluid component, m_f, is obtained by summing Eqs. (2.1.5) through (2.1.8). We will now present the mixture rules and the EOS used in the formulation of an e-relationship for our reacting AP/Al mixture.

2.1.2. Mixture Rules and Equations of State

Here, because it is convenient to express mixture rules in terms of extensive variables, we write E_m and V_m for our AP/Al composition in terms of the extensive internal energies and volumes of its components as

$$E_m = E_{AP}+E_{Al}+E_f+(E_{Al_2O_3}^s)_i \quad i=1 \text{ or } 2 \qquad (2.1.12)$$

$$V_m = V_{AP}+V_{Al}+V_f+(V_{Al_2O_3}^s)_i \quad i=1 \text{ or } 2 \qquad (2.1.13)$$

In this case, the specific internal energy and volume of the mixture are related to E_m and V_m by the equations, $e=E_m/M_0$ and $v=V_m/M_0$. We now introduce the EOS used to calculate the energies on the right-hand side of Eq. (2.1.12).

We write the e=e(p,v) EOS for the condensed components in Gruneisen form as

$$e_{AP} = (\Delta h_f^0)_{AP} + \frac{pv_{AP}}{\Gamma_{AP}} + v_0^{AP} g_{AP}(V) \qquad (2.1.14)$$

$$e_{Al} = \frac{pv_{Al}}{\Gamma_{Al}} + v_0^{Al} g_{Al}(V) \qquad (2.1.15)$$

$$e_{Al_2O_3}^s = (\Delta h_f^0)_{Al_2O_3}^i + \frac{pv_i}{\Gamma_i} + v_0^i g_i(V) \quad i=1 \text{ or } 2 \qquad (2.1.16)$$

In writing these equations, we have used $(\Delta h_f^0)_i$ to denote the specific heat of formation of a species S_i and have reduced their number by using i as a subscript or a superscript with the values 1 and 2, respectively, to denote α-Al_2O_3 and γ-Al_2O_3. In addition the g terms are written as functions of the reduced volume $V=v/v_0$, with the understanding that V in $g_i(V)$ denotes $V=(v/v_0)_i$. The energy terms for the condensed components in Eq. (2.1.12) can readily be obtained by multiplying Eqs. (2.1.14), (2.1.15) and (2.1.16) by the expressions for their respective masses given by Eqs. (2.1.4), (2.1.9), and (2.1.10).

We write the $E_f=E(p,V_f, m_f)$ EOS for the fluid as

$$E_f = m_{H_2O}(\Delta h_f^0)_{H_2O} + V_f\left(\frac{p}{n} - g_f(V)\right), \qquad (2.1.17)$$

where the reduced volume V in g_f at this stage need not be defined. Only the specific heat of formation for H_2O need be included in Eq. (2.1.17) because the heats of formation of all the other fluid constituents are zero. We can now derive a specific energy relationship for our AP/Al mixture as follows.

2.1.3. Derivation of the Specific Energy Relationship

We first derive an expression relating E_m and V_m by substituting the equation for E_f obtained by eliminating V_f between Eqs. (2.1.13) and (2.1.17) into Eq. (2.1.12). The result of these operations leads to the equation

$$E_m = m_{H_2O}(\Delta h_f^0)_{H_2O}+E_{AP}+E_{Al}+(E^s_{Al_2O_3})_i+\left[\frac{P}{n}-g_f(V)\right][V_m-(V_{AP}+V_{Al}+(V^s_{Al_2O_3})_i] \ . \qquad (2.1.18)$$

We then multiply Eqs. (2.1.14)-(2.1.16) for the specific energies e_{AP}, e_{Al}, and $e^s_{Al_2O_3}$ of the condensed components by the expressions for their respective masses in Eqs. (2.1.4). (2.1.9) and (2.1.10) to obtain expressions for E_{AP}, E_{Al}, and $E^s_{Al_2O_3}$, substitute these expressions into Eq. (2.1.18), and collect similar terms. The equations obtained in this way for the heat of formation terms denoted by E_c, the pressure terms denoted by E_p, and the remaining volume terms denoted by E_g are given below.

Collecting the specific heat of formation terms for the components leads to the following equation:

$$E_c = m^0_{AP}(\Delta h_f^0)_{AP}+m^0_{AP}\lambda_1[\alpha_1(\Delta h_f^0)_{H_2O}-(\Delta h_f^0)_{AP}]+\frac{m^0_{Al}}{\beta_1}\lambda_2(\Delta h_f^0)^i_{Al_2O_3}, \quad i=1 \text{ or } 2 \ . \qquad (2.1.19)$$

We now let E_x^0 and Q_1 denote, respectively, the heat of formation of our AP/Al composition and the chemical energy liberated when 1 g of AP decomposes according to R.1. We also let Q_2^i denote the chemical energy liberated when 1 g of Al reacts to form α-Al_2O_3 (i=1) or γ-Al_2O_3 (i=2) according to R.2. We then write Eq. (2.1.19) in terms of these parameters as

$$E_c = E^0_x-m^0_{AP}\lambda_1Q_1-m^0_{Al}\lambda_2Q^i_2 \ . \qquad (2.1.20)$$

Collecting the pressure terms leads to the equation

$$E_p = p\frac{V_m}{n} + \frac{pA_{AP}m_{AP}^0}{n}(1-\lambda_1)v_{AP} + p\frac{A_{Al}}{n}m_{Al}^0(1-\lambda_2)v_{Al} + \frac{pA_i m_{Al}^0}{n\beta_1}\lambda_2 v_i \ , \qquad (2.1.21)$$

where $A_{AP} = (n/\Gamma_{AP}-1)$, $A_{Al} = (n/\Gamma_{Al}-1)$, *and* $A_i = (n/\Gamma_i-1)$.

Collecting the remaining volume terms leads to the equation

$$\begin{aligned} E_g = & -V_m g_f(V) + m_{AP}^0(1-\lambda_1)[v_0^{AP} g_{AP}(V) + v_{AP} g_f(V)] \\ & + m_{Al}^0(1-\lambda_2)[v_0^{Al} g_{Al}(V) + v_{Al} g_f(V)] \\ & + (m_{Al}^0/\beta_1)\lambda_2[v_0^i g_i(V) + v_i g_f(V)] \end{aligned} \qquad (2.1.22)$$

The equation for e for our mixture is obtained by adding Eqs. (2.1.20), (2.1.21), and (2.1.22) and dividing by M_0. Because of space limitations, it serves our purpose here to set g_f=0, and n=k-1 and only present the energy relationship when the products are assumed to be polytropic. In this case, the e-relationship can be written as

$$\begin{aligned} e - e_x^0 = & -\lambda_1 q_1 - \lambda_2 q_2^i \\ & + \frac{p}{k-1}[v + A_{AP}^0(1-\lambda_1)v_{AP} + A_{Al}^0(1-\lambda_2)v_{Al} + A_i^0\lambda_2 v_i] \\ & + a_{AP}^0(1-\lambda_1)g_{AP}(V) + a_{Al}^0(1-\lambda_2)g_{Al}(V) + a_i^0\lambda_2 g_i(V) \ , \end{aligned} \qquad (2.1.23)$$

where $q_1 = \alpha_{AP}^0 Q_1$, $q_2^i = \alpha_{AP}^0 Q_2^i$, $A_{AP}^0 = \alpha_{AP}^0 A_{AP}$, $A_{Al}^0 = \alpha_{Al}^0 A_{Al}$, $A_i^0 = \alpha_{Al}^0 A_i/\beta_1$,

$a_{AP}^0 = \alpha_{AP}^0 v_0^{AP}$, $a_{Al}^0 = \alpha_{Al}^0 v_0^{Al}$, and $a_i^0 = \alpha_{Al}^0 v_0^i/\beta_1$.

At this stage, Eq. (2.1.23) cannot be used to calculate the specific energy of our reacting AP/Al mixture because we have no prescription for calculating the specific volumes of the condensed components when p, v, λ_1, and λ_2 are known. A prescription to address this difficulty will be presented after we have derived the mass balance equations for reacting Al particles in the next section.

2.1.4. The Mass Balance Equations for Al Spheres Reacting with O_2 to Form an Outer Coating of Al_2O_3 and the Reaction Coordinate λ_2.

We consider a shocked sphere of Al with an initial radius r_H, specific volume v_1^H, and mass w_1^0. The initial mass, specific volume and radius of this Al sphere are then related by the equation

$$w_1^0 = \frac{4\pi r_H^3}{3v_1^H} \ . \qquad (2.1.24)$$

We then assume that a mass fraction of Al, λw_1^0, has reacted with the O_2 in the surroundings to produce a sphere of radius R. This sphere consists of an outer shell of Al_2O_3 with mass w_2^i, specific volume v_2^i and a thickness l^i, that covers an inner core of Al with a radius R-l^i. In this case, the mass of Al in the inner core, w_1, satisfies the equations

$$w_1 = \frac{4\pi(R-l^i)^3}{v_1} = \frac{4\pi r_H^3}{3v_1^H}(1-\lambda) , \qquad (2.1.25)$$

which gives the following equation for λ:

$$\lambda = 1 - \frac{v_1^H}{v_1}\left(\frac{R-l^i}{r_H}\right)^3 . \qquad (2.1.26)$$

We note that Eq. (2.1.26) satisfies the conditions, $\lambda_H=0$, when $l^i=0$ and $R=r_H$, and $\lambda=1$ when the thickness of the Al_2O_3 coating equals the radius of the sphere. We now use the mass balance equation from R.2 to derive another equation for R and thereby obtain the relationship between l^i and λ. We accordingly integrate the equation obtained by setting $m_{Al}=w_1$, $M_{al}=M_1$, $m^i_{Al_2O_3}=w_2^i$, and $M_{Al_2O_3}=M_2$ in Eq. (2.1.2) to obtain the following equations relating w_1 and w_2:

$$w_1^0 - w_1 = 2M_1\xi_2 \qquad (2.1.27)$$

$$w_2^i = M_2\xi_2 \qquad (2.1.28)$$

Eliminating ξ_2 between Eqs (2.1.27) and (2.1.28) then gives the equation

$$\lambda w_0 = (2M_1/M_2)\, w_2^i, \qquad (2.1.29)$$

which we rewrite as

$$\lambda\frac{4\pi r_H^3}{3v_1^H} = \frac{2M_1}{M_2}\,\frac{4\pi}{3}\,\frac{R^3-(R-l^i)^3}{v_2^i} . \qquad (2.1.30)$$

The combination of Eqs. (2.1.26) and (2.1.30) then leads to the following equation relating R and λ:

$$R = r_H\left[\frac{V_2^i}{2V_1^H}\lambda + \frac{V_1}{V_1^H}(1-\lambda)\right]^{1/3} , \qquad (2.1.31)$$

where $V_1=v_1M_1$ denotes the molar volume of Al and $V_2^i=v_2^i, M_2$ denotes the molar volume of Al_2O_3. Setting $\lambda=1$ in Eq. (2.1.31) gives the final radius of the sphere when all the Al has reacted to form Al_2O_3. The combination of Eqs. (2.1.26) and (2.1.31) then gives the equation relating l^i and λ as

$$\frac{l^i}{r_H} = \left[\frac{V_2^i}{2V_1^H}\lambda + \frac{V_1}{V_1^H}(1-\lambda)\right]^{1/3} - \left(\frac{V_1}{V_1^H}\right)^{1/3}(1-\lambda)^{1/3} . \qquad (2.1.32)$$

Having introduced the reaction coordinate λ for a single Al particle, we must now relate this coordinate to the global coordinate λ_2 defined by the equation $m_{Al}=m^0_{Al}(1-\lambda_2)$. For simplicity, we will assume that our AP/Al mixture contains N_{Al} particles of Al with the same initial radius r_0, and write the equation for m^0_{Al} as $m^0_{Al}=N_{Al}4\pi r_0^3/3v_0^{Al}$. We now multiply Eq. (2.1.25) by N_{Al} to

obtain the total amount of unreacted Al in our mixture, when the covering layers of Al_2O_3 have a thickness l^i, as

$$m_{Al} = N_{Al} w_1 = \frac{4\pi N_{Al} r_H^3}{3 v_1^H} (1-\lambda) . \qquad (2.1.33)$$

The mass balance condition $(r_0^3/v_0^{Al}) = (r_H^3/v_1^H)$ then allows us to rewrite Eq. (2.1.33) as $m_{Al}=m_{Al}^0(1-\lambda)$ and show that $\lambda=\lambda_2$ when all the Al particles in our AP/Al mixture are assumed to have the same size.

2.1.5. Implementation of the e-Relationship.

Our prescription to make Eq. (2.1.23) into a working relationship is based on the premise that the components of our reacting AP/Al mixture do not attain thermal equilibrium during the detonation process. Consequently, because an explicit treatment of heat conduction is beyond the scope of Phase I tasks, addtional assumptions must be made about the transfer of heat among these components. Here, we will treat the AP and Al in a similar way, and assume that no appreciable amount of heat is transferred into either the interior of a burning AP grain or the interior of a reacting Al particle, as the reacting AP/Al mixture expands. In this case, a grain of AP and a particle of Al entering the shock are thereafter constrained to their respective isentropes determined by their thermodynamic states attained at the shock front. In contrast to this treatment of AP and Al, we assume that the heat transfer process between Al_2O_3 and the fluid component as so efficient that the Al_2O_3 coatings on the Al particle attain thermal equilibrium with the decomposition products of the AP. The consequences of these assumptions, which make Eq. (2.1.23) a workable e-relationship will be considered later.

2.2 A Specific Energy Relationship for a Reacting $C_aH_bN_cO_d$/Al Mixture.

Our formulation of an e-relationship for a $C_aH_bN_cO_dAl_f$ composition follows a procedure similar to that used in our formulation of the e-relationship for AP/Al mixture. To be more specific, we adopt the assumption A.3, apply assumption A.4 to the $C_aH_bN_cO_dAl_f$ system, and make the following assumptions about the decomposition of the explosive $C_aH_bN_cO_d$, and the reactions of its products with the Al:

A.5 The $C_aH_bN_cO_d$ explosive decomposes to give products with a fixed composition, as prescribed, by Kamlet[8].

A.6 The Al reacts with the CO_2 and H_2O produced by $C_aH_bN_cO_d$, and the H_2 liberated from the H_2O reacts with the C in the explosive's products to form hydrocarbons.

2.2.1. Mass Balance Equations for a $C_aH_bN_cO_dAl_f$ Composition

We again consider a mass M_0=100g of explosive mixture with an initial mass fraction of X, $\alpha_x^0=m_x^0/M_0$, and an initial mass fraction of Al, $\alpha_{Al}^0=m_{Al}^0/M_0$. It is clear for this X/Al mixture that $m_{Al}^0=fM_{Al}$ and that $m_x^0=M_0-fM_{Al}$. Following Kamlet, we write the equation for the decomposition of our explosive component as

$$C_aH_bN_cO_dAl_f \rightarrow b_1H_2O+a_1CO_2+c_1N_2+a_2C+fAl \qquad (R.3)$$

with $b_1=b/2$, $a_1=d/2-b/4$, $c_1=c/2$, and $a_2=a-(d/2-b/4)$. To consider the heat produced by (R.3), we denote the heat of formation of a mole of a species S as $(\Delta H_f^0)_s$ and write the standard heat of decomposition of X in the composition, Q_x, as

$$Q_x = -[b_1(\Delta H_f^0)_{H_2O}+a_1(\Delta H_f^0)_{CO_2}-(\Delta H_f^0)_x] \ . \qquad (2.2.1)$$

and its specific heat of decomposition as

$$q_x = -\frac{1}{M_x}[b_1M_{H_2O}(\Delta h_f^0)_{H_2O}+a_1M_{CO_2}(\Delta h_f^0)_{CO_2}-M_x(\Delta h_f^0)_x] \ . \qquad (2.2.2)$$

because $M_x=m_x^0$.

We now consider the reactions of Al with the explosive's products. We write the equation for the Al in the composition reacting with the CO_2 as

$$fAl+\frac{3f}{2}CO_2 = \frac{f}{2}Al_2O_3+\frac{3}{2}fCO \ . \qquad (R.4)$$

Examination of (R.3) and (R.4) then shows that all the Al in the composition can react with the CO_2 when $a_1 \geq 3f/2$. We write the equation for the Al in the composition reacting with the H_2O as and similarly see that the condition for all the Al to react with the H_2O is $b_1 \geq 3f/2$. Because (R.5)

$$fAl+\frac{3f}{2}H_2O = \frac{f}{2}Al_2O_3+\frac{3}{2}fH_2 \qquad (R.5)$$

produces H_2, we must also consider the reaction of the H_2 with the C produced by the explosive. For simplicity, we only consider one reaction between H_2 and C and write this reaction as

$$\frac{3}{2}fH_2+fC = \frac{f}{2}C_2H_6 \qquad (R.6)$$

Examination of (R.3) and (R.6) then shows that the condition for all the hydrogen produced by the H_2O to react with the C is $a_2>f$. On the added assumption that the H_2 produced by the H_2O reacts immediately with the C produced by the explosive, we combine (R.5) and (R.6) and write the equation for this Al-H_2O-C reaction as

$$fAl+\frac{3}{2}fH_2O+fC = \frac{f}{2}(Al_2O_3)_s^i+\frac{f}{2}C_2H_6 \qquad (R.7)$$

and the equation for its standard heat of reaction, Q_{Al}, as

$$Q_{Al}^i = -\frac{f}{2}[(\Delta H_f^0)_{C_2H_6}+(\Delta H_f^0)_{Al_2O_3}^i-3(\Delta H_f^0)_{H_2O}] \qquad (2.2.3)$$

To be more specific about such X-Al compositions, we consider a composition similar to H6 with a=1.8869, b=2.6123, c=1.5796, d=1.9667, and f=0.7827. Because $a_1=0.3303$ and $3f/2=1.1740$, we see that $3f/2>a_1$ for this composition, and X does not produce enough CO_2 to consume all the Al. Alternatively, because $b_1=1.3061>3f/2$, and $a_2=1.5566>f$, the H_2O produced by X can consume all the Al, and the C produced by X can react with all the H_2 product from the H_2O by (R.3). For these reasons, it is convenient here to neglect the reaction of Al and CO_2 in

this composition and only consider the two global exothermic reactions, (R.3) and (R.7).

In order to account for (R.3) and (R.7) in the detonation process, we introduce the extent ξ_3 for (R.3), the extent of reaction ξ_7 for (R.7), and write the law of definite proportions for these reactions as

$$-\frac{dm_x}{M_x} = \frac{dm^3_{H_2O}}{b_1 M_{H_2O}} = \frac{dm_{N_2}}{c_1 M_{N_2}} = \frac{dm_{CO_2}}{a_1 M_{CO_2}} = \frac{dm^3_C}{a_2 M_C} = d\xi_3 \tag{2.2.4}$$

$$-\frac{dm^7_C}{fM_C} = -\frac{dm_{Al}}{fM_{Al}} = -\frac{dm^7_{H_2O}}{\frac{3}{2}fM_{H_2O}} = \frac{dm^i_{Al_2O_3}}{\frac{1}{2}fM_{Al_2O_3}} = \frac{dm_{C_2H_6}}{\frac{1}{2}fM_{C_2H_6}} = d\xi_7 \,. \tag{2.2.5}$$

with

$$dm_{H_2O} = dm^3_{H_2O} + dm^7_{H_2O} \tag{2.2.6}$$

$$dm_C = dm^3_C + dm^7_C \tag{2.2.7}$$

Formally integrating these equations, setting $\xi_3=\lambda_3$ and $\xi_7=\lambda_7$, and introducing the mass fractions

$$\alpha_1 = \frac{c_1 M_{N_2}}{m^0_x}\,,\ \alpha_2 = \frac{b_1 M_{H_2O}}{m^0_x}\,,\ \alpha_3 = \frac{a_1 M_{CO_2}}{m^0_x}\,,\ \alpha_4 = \frac{a_2 M_C}{m^0_x}\,,$$

allows us to write the equations for the masses of the species in our reactive X/Al mixture as

$$m_x = m^0_x(1-\lambda_3) \tag{2.2.8}$$

$$m_{N_2} = m^0_x \alpha_1 \lambda_3 \tag{2.2.9}$$

$$m_{CO_2} = m^0_x \alpha_3 \lambda_3 \tag{2.2.10}$$

$$m_{H_2O} = m^0_x \alpha_2 \lambda_3 - \frac{3}{2} fM_{H_2O}\lambda_7 \tag{2.2.11}$$

$$m_C = m^0_x \alpha_4 \lambda_3 - fM_C\lambda_7 \tag{2.2.12}$$

$$m_{C_2H_6} = \frac{f}{2} M_{C_2H_6}\lambda_7 \tag{2.2.13}$$

$$m_{Al} = m^0_{Al}(1-\lambda_7) \tag{2.2.14}$$

$$m^i_{Al_2O_3} = \frac{f}{2} M_{Al_2O_3}\lambda_7 \tag{2.2.15}$$

The Eqs. (2.2.8), (2.2.14), and (2.2.15), respectively, give the masses of the condensed components X, Al, and Al_2O_3 in terms of the reaction coordinates, and the equation for the mass of the other species can be obtained by summing Eqs. (2.2.9) through (2.2.13) as

$$m_p = m^0_x \lambda_3 - f\,(\frac{3}{2}M_{H_2O} + M_c - \frac{M}{2}C_2H_6)\lambda_7 \,. \tag{2.2.16}$$

To simplify our treatment here, but account for the presence of solid C in the detonation products, we make the additional assumption that the species CO_2, H_2O, N_2, and C_2H_6 form a

polytropic fluid mixture with an index k and that C is a polytropic solid with the same index. We can then proceed with our formulation of an e-relationship for our X/Al mixture.

2.2.2. Mixture Rules and Equations of State (EOS)

We again use E_m and V_m to denote the internal energy and volume of our X/Al composition, and express E_m and V_m in terms of the internal energies and volumes of its components as

$$E_m = E_x+E_f+E_{Al}+(E^s_{Al_3O_3})_i \tag{2.2.17}$$

We then write the e=e(p,v) equation of state (EOS) of the explosive as

$$V_m = V_x+V_f+V_{Al}+(V^s_{Al_3O_3})_i \ . \tag{2.2.18}$$

$$e_x = (\Delta h^0_f)_x+\frac{pv_x}{\Gamma_x}+v^x_0 g_x(V) \ , \tag{2.2.19}$$

use Eqs. (2.1.15) and (2.1.16) to describe Al and Al_2O_3, and write the E_f=E(p,V_f, m_j) EOS for our products' component as

$$E_f = \Sigma_j m_j(\Delta h^0_f)_j+\frac{pV_f}{\gamma-1} \ , \tag{2.2.20}$$

with j=CO_2, H_2O, C_2H_6, and m_{CO_2} , m_{H_2O} , *and* $m_{C_2H_6}$ defined by Eqs. (2.2.10), (2.2.11), and (2.2.13). Our derivation of a specific energy relationship for the X/Al mixture now parallels that for the AP/Al mixture.

2.2.3. Derivation of the Specific Energy Relationship

We first derive an expression relating E_m and V_m by substituting the equation for E_f, obtained by eliminating V_f between Eqs. (2.2.18) and (2.2.10), into Eq. (2.2.17). These operations give

$$E_m = (E_x-\frac{pV_x}{\gamma-1}) + (E_{Al}-\frac{pV_{Al}}{\gamma-1}) + (E^s_{Al_2O_3}-\frac{pV^s_{Al_2O_3}}{\gamma-1})_i + \Sigma m_j(\Delta h^0_f)_j+\frac{pV_m}{\gamma-1} \ . \tag{2.2.21}$$

We then multiply Eqs. (2.2.19), (2.1.15), and (2.1.16), for the specific internal energies of the condensed components, by the expressions for their respective masses given in Eqs. (2.2.8), (2.2.14), and (2.2.15), to obtain expressions for E_x, E_{Al}, and $(E^s_{Al_2O_3})_i$, substitute these expressions into Eq. (2.2.21), and collect similar terms. The resulting equations for the heat of formation terms denoted by E_c, the pressure terms denoted by E_p, and the remaining volume terms denoted by E_g are given below.

The equation for E_c is obtained as

$$E_c = E^0_x-Q_x\lambda_3-Q^i_{Al}\lambda_7 \ , \tag{2.2.22}$$

with E^0_x=$m^0_x(\Delta h^0_f)_x$ because $(\Delta h^0_f)_{Al}$=0. The equation for E_p is obtained as

$$E_p = \frac{p}{\gamma-1}[V_m + A_x m_x^0(1-\lambda_3)v_x + A_{Al} m_{Al}^0(1-\lambda_7)v_{Al} + A_i \frac{f}{2} M_{Al_2O_3}\lambda_7 v_i] \ , \qquad (2.2.23)$$

with $A_x = \frac{\gamma-1}{\Gamma_x} - 1$, $A_{Al} = \frac{\gamma-1}{\Gamma_{Al}} - 1$, *and* $A_i = \frac{\gamma-1}{\Gamma_i} - 1$ defined previously for the AP/Al composition. The equation for E_g is obtained as

$$E_g = V_0^x(1-\lambda_3)g_x(V) + V_0^{Al}(1-\lambda_7)g_{Al}(V) + \frac{f}{2} M_{Al_2O_3} v_0^i \lambda_7 g_i(V) \ , \qquad (2.2.24)$$

with $V_o^x = m_x^0 v_o^x$ *and* $V_0^{Al} = m_{Al}^0 v_0^{Al}$.

Finally, adding Eqs. (2.2.22), (2.2.23), and (2.2.24) together and dividing the resulting equation by M_0, gives the e-relationship for our X/Al mixture as

$$\begin{aligned} e - e_x^0 = \quad & -q_3\lambda_3 - q_{Al}^i\lambda_7 \\ & + \frac{p}{\gamma-1}[v + A_x^0(1-\lambda_3)v_x + A_{Al}^0(1-\lambda_7)v_{Al} + A_i^0\lambda_7 v_i] \\ & + [a_x^0(1-\lambda_3)g_x(V) + a_{Al}^0(1-\lambda_7)g_{Al}(V) + a_i^0\lambda_7 g_i(V)] \end{aligned} \qquad (2.2.25)$$

with

$$q_3 = \alpha_x^0 q_x \ , \ q_{Al}^i = Q_{Al}^i/M_0 \ , \ A_x^0 = A_x\alpha_x^0 \ ,$$
$$A_{Al}^0 = A_{Al}\alpha_{Al}^0 \ , \ A_i^0 = A_i f\, M_{Al_2O_3}/2M_0 \ ,$$
$$a_x^0 = \alpha_x^0 v_0^x \ , \ a_{Al}^0 v_0^{Al} \ , \ a_i^0 = fM_{Al_2O_3} v_0^i/2M_0 \ .$$

Having derived e-relatinships for AP/Al and X/Al mixtures in terms of general MG EOS, we must now formulate the particular EOS that are needed for their implementation.

2.3 Equations of State for the Components in AP/Al and X/Al Compositions.

Because Al is present in both of our explosive compositions, we will formulate an EOS for Al before considering the EOS of the other components.

2.3.1. A Complete Equation of State for Al

Difficulties arise in modeling the reactions of a metal with an explosive's products behind the detonation front when the EOS of the metal is based on shock wave data and is, consequently, valid only for values of the specific volume v, $v \le v_0 = \rho_0^{-1}$, where ρ denotes the density and the subscript o denotes the unshocked state. An approach to resolve this difficulty, which is different from the one presented here, has been formulated by J.W. Enig[9]. To be more specific about this difficulty, we consider an e=e(p,v) EOS based on the assumption that the Gruneisen parameter Γ is only a function of v. (The thermodynamic conditions for this assumption to be valid will be presented later.) In this case,

$$(\partial e/\partial p)_v = v/\Gamma(v), \qquad (2.3.1)$$

and the e=e(p,v) relation follows by formally integrating Eq. (2.3.1), yielding

$$e = pv/\Gamma(v)+g(v), \tag{2.3.2}$$

where g(v) is an arbitrary function of v. When $\Gamma(v)$ is known, the knowledge of $e_R(v)$ along a reference curve $p_R = p_R(v)$ in the (v-p) plane allows us to determine g(v) over the volume range, $v_1 \le v \le v_2$, spanned by $p_R(v)$ and to rewrite Eq. (2.3.2) as

$$e-e_R(v) = (p-p_R(v))v/\Gamma(v) \text{ for } v_1 \le v \le v_2. \tag{2.3.3}$$

Because shock wave studies of a material provide its Hugoniot curve in the (v-p) plane,

$$p_H = p_H(v,v_0) \text{ for } v \le v_0, \tag{2.3.4}$$

and because the energy change along a Hugoniot curve is defined by the Hugoniot relation

$$2(e_H-e_0) = p_H(v_0-v), \tag{2.3.5}$$

it is convenient to write an e=e(p,v) EOS calibrated with shock wave data as

$$e-e_H = (p-p_H)v/\Gamma(v). \tag{2.3.6}$$

When writing an e=e(p,v) EOS in this form, one must remember that its validity is limited strictly to the volume range, $v \le v_0$, spanned by the $p_H=p_H(v,v_0)$ Hugoniot curve.

To provide more background for our EOS task, we now discuss Debye's approach to solids to establish thermodynamic conditions for Γ to be a function of v.

2.3.1.1. Thermodynamics of a Debye Solid

We let T and $u_0(v)$ denote, respectively, the absolute temperature and the specific internal energy along the zero degree (T=0 K) isotherm, and write the equation for the specific Helmholtz free energy f as

$$f = u_0(v)+TF(\Theta/T), \tag{2.3.7}$$

where the Debye temperature Θ is assumed to be a function only of v and is related to the maximum frequency that can be propagated in the lattice ω_k, by the equation $\Theta=(h/k)\omega_m/2\pi$. Equation (2.3.7) is used to derive an equation for Γ/v, rewritten as

$$\Gamma/v = (\partial p/\partial T)_v/C_v, \tag{2.3.8}$$

where C_v denotes the specific heat at constant volume.

To obtain the equation for $(\partial p/\partial T)_v$, we first differentiate Eq. (2.3.7) partially with respect to v to obtain the following equation for p:

$$p = p_0(v) - F'd\Theta/dv \tag{2.3.9}$$

where $p_0(v)=-du_0/dv$ denotes the pressure along the zero degree isotherm and $F'=dF/d(\Theta/T)$. We then differentiate Eq. (2.3.9) partially with respect to T to obtain the equation for $(\partial p/\partial T)_v$ as

$$(\partial p/\partial T)_v = (\Theta F''/T^2)d\Theta/dv \tag{2.3.10}$$

with $F''=d^2F/d(\Theta/T)^2$. To obtain the equation for C_v, we differentiate Eq. (2.3.7) twice with respect to T to obtain the following equations for the specific entropy s and its derivative $(\partial s/\partial T)_v$,

$$s = -F+(\Theta/T)F' \tag{2.3.11}$$

$$(\partial s/\partial T)_v = -(\Theta^2/T^3)F'' \tag{2.3.12}$$

and we then use the identity $T(\partial s/\partial T)_v=C_v$ to obtain the equation for C_v as

$$C_v=-(\Theta/T)^2F'' \tag{2.3.13}$$

The combination of Eqs. (2.3.8), (2.3.10), and (2.3.13) then gives the equation for Γ as

$$\Gamma = -(v/\Theta)d\Theta/dv, \tag{2.3.14}$$

which shows that Γ is a function only of v.

The assumption that Γ is a function of v is thus valid when the contribution of the lattice vibrations to f are realistically accounted for by the dependence of the Debye temperature Θ on v.

To complete our thermodynamic discussion of EOS with $\Gamma=\Gamma(v)$, we combine the identity e=f+Ts and Eqs. (2.3.7), (2.3.9), (2.3.11), and (2.3.14) to derive the e=e(p,v) EOS for a Debye solid as follows. We first substitute Eqs. (2.3.7) and (2.3.11) into the identity for e to obtain the equation

$$e=u_0(v) + \Theta F', \tag{2.3.15}$$

which is the complete e=e(s,v) EOS for the solid because Θ is only a function of v and s is only a function of Θ/T. We combine Eq. (2.3.11) with the Eqs. (2.3.9) and (2.3.4) to obtain the e=e(p,v) relation as

$$e = u_0(v) + (p-p_0(v))v/\Gamma \tag{2.3.16}$$

Comparing Eqs. (2.3.16) and (2.3.3), then shows that the natural reference curve in the (v-p) plane for the Debye solid is the zero degree isotherm, and comparing Eqs. (2.3.16) and (2.3.2) shows that the function g(v) for the Debye solid is

$$g(v) = u_0(v) - \Theta^{-1}(dv/d\Theta)du_0/dv \tag{2.3.17}$$

2.3.1.2. Approach to the EOS Task

Our approach to formulate a realistic EOS for Al for detonation calculations was based on two observations. The first observation is that to a good approximation, for Al subject to the ranges of pressures and temperatures of interest, C_v is constant and the Gruneisen parameter has a constant value Γ=2. The second observation is that D.J. Pastine[10] had considerable success calculating shocked states in face-centered cubic metals by using a Morse potential to represent their zero degree isotherms. This Morse potential can be written for a gram atomic weight of metal in terms of the distance paramter $y=1-(v/v_0)^{1/3}$, with v_0 used to denote v at 0°K, a parameter b, and the latent heat of sublimation U_0 as

$$\hat{U}(v/v_0) = U_0(\exp(2by)-2\exp(by)) \qquad (2.3.18)$$

Our approach, based on these observations, can be stated as follows. Use the values C_v=0.221 cal/g, Γ=2, and shock wave data for Al, and the Morse potential to generate reference curves $e_R=e_R(v)$ and $p_R=p_R(v)$ and, thereby, construct an EOS for Al that is not restricted to the volume range spanned by its Hugoniot curve $p_H=p_H(v,v_0)$.

It was thought necessary, in implementing this approach, to construct an EOS for Al in the region spanned by its Hugoniot curve, and then ascertain the thermodyanic compatability of this EOS with the Morse potential. To provide the background for this implementation, we first present a method for using shock wave data to construct a complete EOS for a material with constant values of C_v and Γ. We then present our procedure for testing the compatibility of this EOS and the Morse potential.

After completing this background, the application of our approach to Al is given.

2.3.1.3. A Complete EOS Based on Shock Wave Data

For our present purpose, it is convenient to consider a complete EOS as an EOS that allows us to calculate the values of e, T, and s at a point in the (v-p) plane. In this case, when C_v and Γ are known constants, we claim that knowledge of the Hugoniot curve $p_H=p_H(v,v_0)$ through the initial state (v_0, p_0, e_0, s_0, T_0) provides enough information to construct a complete EOS in the region of the (v-p) plane spanned by $p_H=p_H(v,v_0)$ above the T_0 isotherm. We substantiate this claim as follows.

For convenience, we assume that the $p_H=p_H(v,v_0)$ curve satisfies the equation

$$p_H = a^2(v_0-v)/(v_0-B(v_0-v))^2 \qquad (2.3.19)$$

obtained from a linear shock velocity U-particle velocity u relation, U=a+Bu, and then consider the following differential equation for shock temperature T_H,

$$dT_H+(\Gamma/v)T_H dv = (2C_v)^{-1}[(v_0-v)dp_H+p_H dv] \qquad (2.3.20)$$

obtained by equating the differential de_H calculated from the e=e(T,v) EOS and Eq. (2.3.5). Formally, integrating Eq. (2.3.20) gives the equation for T_H as

$$T_H = T_0(\frac{v_0}{v})^{\Gamma} + (2C_v v^{\Gamma})^{-1}\int_{v_0}^{v} v^{\Gamma}[(v_0 - v)(\frac{dp_H}{dv}) + p_H]dv \ , \qquad (2.3.21)$$

which shows that the shock temperature can be calculated along the Hugoniot curve $p=p_H(v,v_0)$ when p_H is a known function of v, as exemplified by Eq. (2.3.19).

After T_H has been calculated as a function of v, the equation

$$C_v\Gamma(T-T_H) = v(p-p_H) \qquad (2.3.22)$$

can be used to calculate temperature along isochores emanating from the T_0 isotherm. Because e can also be calculated along these isochores from Eq. (2.3.6) when Γ is a known constant, we need finally, to derive an equation for calculating s. Consequently, we integrate the differential ds obtained from the s=s(T,v) EOS, to obtain the following equation for the entropy along the Hugoniot curve,

$$s_H = s_0 + C_v[\ln(T_H/T_0) + \Gamma\ln(v/v_0)], \qquad (2.3.23)$$

and write the equation for the entropy along isochores emanating from $p_H=p_H(v,v_0)$ as

$$s = s_H + C_V \ln(T/T_H) \qquad (2.3.24)$$

Combining Eqs. (2.3.23) and (2.3.24) then gives the equation for calculating the entropy as

$$s = s_0 + C_v[\ln(T/T_0) + \Gamma\ln(v/v_0)] \qquad (2.3.25)$$

It is now convenient to write the equations for the isotherm and the isentrope through the initial state $(v_0,p_0=0)$ because we may use the Morse potential to try to match one of these curves later. Setting $T=T_0$ in Eq. (2.3.22) gives the equation for the T_0 isotherm in the (v-p) plane as

$$p = p_H - (T_H - T_0)\, C_v\Gamma/v \qquad (2.3.26)$$

And substituting into Eq. (2.3.22) the expression for T obtained by setting $s=s_0$ in Eq. (2.3.25), gives the equation for the isentrope through the initial state $(v_0,p_0=0)$ as

$$p = p_H - [T_H - T_0\,(v_0/v)^{\Gamma}]C_v\Gamma/v \qquad (2.3.27)$$

2.3.1.4. The Compatability Condition for the Morse Potential and an EOS Calibrated with Shock Wave Data

Because Eq. (2.3.18) for the Morse potential was originally written for the 0 K isotherm and the specific volume of metals at 0 K and p=0 are not really known, we will use this equation here with v_0 considered to be the specific volume in the unshocked state. In this case, U_0 is the latent heat of sublimation at T_0. We assume that Eq. (2.3.18) represents the energy along an adiabat so that the equation for the isentrope passing through $(v_0, p=0)$ is obtained by differentiating Eq. (2.3.18) with respect to v as

$$p = -(d\hat{U}/dy)(dy/dv) \qquad (2.3.28)$$

and p=0 when $d\hat{U}/dy=0$ and $v=v_0$. Our compatability condition for the Morse potential and an EOS based on shock wave data is that, for the pressure range of interest, we can find a value of b for which the values of p calculated along the isentrope defined by Eq. (2.3.28) match those calculated along the isentrope defined by Eq. (2.3.27).

2.3.1.5. Application of This Approach to Al

In order to determine if the Morse potential can be incorporated into the EOS for Al based on shock wave data, values of the pressure calculated for Al using Eq. (2.3.27) must be compared with the corresponding values of pressure calculated from Eqs. (2.3.18) and (2.3.28). To this end, we first use these equations to calculate values of the pressure along the isentrope passing through (v_0, p=0)

Because shock temperature must be known before we can use Eq. (2.3.27), we first use Eq. (2.3.19) to evaluate the integral, say I, on the right-handed-size of Eq. (2.3.21), and thereby obtain an equation for calculating T_H along the Hugoniot curve. Because $\Gamma=2$, this integral I can be written in closed form as the sum of three terms, $I = I_1+I_2+I_3$, with I_1, I_2, and I_3 expressed in terms of $V=v/v_0$ and $\bar{V}= (1-B)+BV$, as

$$I_1 = p_H v_0^3 \bar{V}^2(1-\bar{V}) \qquad (2.3.29.1)$$

Equations (2.3.21) and (2.3.29.1) through (2.3.29.3) were used with the appropriate values of

$$I_2 = \frac{2(av_0)^2}{B^3}[(\bar{V}-1)-(2-B)\ln\bar{V}+(B-1)((\bar{V})^{-1}-1)] \qquad (2.3.29.2)$$

$$I_3 = (\frac{2av_0}{B^2})^2[0.5(1-\bar{V}^2)+(3-2B)(\bar{V}-1)+(3-B)(B-1)\ln\bar{V}-(B-1)^2((\bar{V})^{-1}-1)] \qquad (2.3.29.3)$$

$v_0=0.3584$ cm^3/g, a=5.33 mm/μsec, and B=1.34 for Al to calculate values of T_H in the reduced volume range, $0.77 \le V \le 1$. These values of T_H and the corresponding values of p_H were then used in Eq. (2.3.27) with T_0=298K to calculate values of the pressure p_s along the (v_0, p=0) isentrope. The energy change along this isentrope, $e_s - e_0$, was also calculated using Eq. (2.3.6) with $\Gamma=2$. The values of T_H, p_H, and p_s and $e_s - e_0$, calculated in this way are listed in Table 2.1. The following equation for the (v_0, p=0) isentrope, obtained from the first law of thermodynamics as

$$p_s v^2 = -2\int_{v_0}^{v} v^2(\frac{dg}{dv})dv \ , \qquad (2.3.30)$$

with

$$g(\bar{V}) = (\frac{a}{B})^2[1-\frac{1+B}{\bar{V}}+\frac{B}{\bar{V}^2}] \ , \qquad (2.3.31)$$

was also used to calculate values of p_s at the same values of V to provide a check on the shock

temperature calculations. Both of these sets of values for p_s were found to be in excellent agreement.

The equation for calculating p_s from the Morse potential follows from Eqs. (2.3.18) and (2.3.28) as

$$p_s = \frac{2b\rho_0 U_0}{3V^{2/3}}[\exp(2by)-\exp(by)] \; ; \qquad (2.3.32)$$

the equation for the slope of this isentrope is obtained by differentiating Eq. (2.3.32) with respect to v, yielding

$$-v_0^2 \frac{dp_s}{dv} = \frac{4bU_0}{9V^{5/3}}[\exp(2by)-\exp(by)] + \frac{2b^2U_0}{9V^{4/3}}[2\exp(2by)-\exp(by)] \qquad (2.3.33)$$

Recalling that the isentrope and the Hugoniot curve are tangent at (v_0, p=0), we then equate their initial slope $(dp_H/dv)_0=-(a/v_0)^2$ to that obtained by setting y=0 in Eq. (2.3.33) to obtain the following equation for the parameter b:

$$b^2 = 9a^2/2U_0 \qquad (2.3.34)$$

Because the listed value of U_0 for Al at 298°K is 78 kcal/mol, and a=5.33 mm/μsec, we are forced to use the value of b=3.25 when calculating p_s from Eqs. (2.3.32). The values of p_s and e_s-e_0 calculated from Eqs. (2.3.32) and (2.3.18) using these values for the parameters are also listed in Table 2.1.

We now compare the two sets of values for p_s and e_s-e_0 listed in Table 2.1 to see if the Morse potential is thermodynamically compatable with our EOS for Al based on shock wave data. The excellent agreement between these two sets of values for p_s and e_s-e_0 shows that the Morse potential can be used for Al to define realistic values for the reference energy $e_R=\hat{U}(v)$ along the reference curve $p_R = p_s(v) = -d\hat{U}/dv$ in pressure regions of interest. In this case, we can write Eq. (2.3.2) for Al with Γ=2 and the function g(v) defined by the Morse potential as

$$e = pv/2 + \hat{U}(v/v_0) - p_s v/2 \qquad (2.3.35)$$

The equation for p_H can then be obtained by combining Eqs. (2.3.35) and (2.3.5) as

$$p_H = (p_s V + 2(e_0 - \hat{U}(v/v_0))\rho_0)/(2V-1), \qquad (2.3.36)$$

and Eq. (2.3.27) with $p=p_s$ can be used to calculate T_H. The values of p_H and T_H calculated from the Morse potential in this way are also listed in Table 2.1.

Table 2.1. Values of the shock pressure p_H, the shock temperature T_H, and the pressure p_s and change in specific internal energy e_s-e_0 along the (v_0, p=0) isentrope calculated for different values of the reduced volume V=v/v_0 from an EOS for Al based on shock wave data and from the Morse potential with U_0=78 kcal/mol and b=3.25.

	EOS Values				**Morse Potential Values**			
V	p_H kbar	T_H K	e_s-e_0 (mm/μ)^2	p_s kbar	p_s kbar	e_s-e_0 (mm/μ)^2	T_H K	p_H kbar
1.00	0.0	298.0	0.0000	0.0	0.0	0.0000	298.0	0.0
0.95	45.5	332.2	0.0391	45.4	45.3	0.0399	332.0	45.4
0.90	105.7	387.1	0.1733	104.7	104.2	0.1706	387.1	105.3
0.85	186.2	495.5	0.4243	181.2	180.9	0.4234	494.8	185.9
0.80	295.8	712.4	0.8322	279.9	281.0	0.8325	718.3	297.3
0.77	380.9	933.6	1.1713	352.0	355.6	1.1725	954.8	385.9

After comparing the corresponding sets of values for the thermodynamic variables listed in Table 2.1, we conclude that the Morse potential provides a realistic description of Al for our detonation calculations.

2.3.2 An Equation of State For AP Based on Shock Wave Data.

Because AP is expected to decompose completely in the early stages of the detonation process, we use Eq. (2.3.6) to write its e=e(p,v) EOS as

$$e=e_H+(p-p_H)v/\Gamma(v).$$

In this case, when the e=e(p,v) EOS is rewritten in the form given by Eq. (2.1.14) as

$$e_{AP} = (\Delta h_f^0)_{AP} + \frac{pv_{AP}}{\Gamma_{AP}} + v_0^{AP} g_{AP}(V)$$

The function $g_{AP}(V)$ is defined over the volume spanned by the Hugoniot curve passing through the initial state ($v=v_0$, p=0, $e=e_0$). A method of extending this volume range is presented in Section 2.3.3.

Our construction of an e=e(p,v) EOS for AP is based on the shock-wave data for AP given by F.W. Sandstrom, P.A. Persson, and B. Olinger (SPB)[11], and its thermodynamic data given in the LLNL Explosives Handbook[12]. To be more specific, SPB give the following Hugoniots for solid density AP (ρ_0=1.95 g/cm^3), U=2.84+1.85u for $0.21 \le u \le 0.50$ and U=2.90+1.59u for $0.66 \le u \le 2.10$, as well as the value for the bulk sound velocity c_0=2.84 mm/μsec; the LLNL Handbook gives the estimated values for the specific heat at constant pressure C_p, and the linear expansion coefficient $\alpha=l^{-1}(\partial l/\partial T)_p$ as C_p=0.31 cal/g°C and $\alpha \approx 40\times10^{-6}$/°C. Substituting these values for C_p and c_0 into the thermodynamic identity

$$\Gamma = \frac{c_0^2}{c_p v}\frac{\partial v}{\partial T_p} \tag{2.3.37}$$

and the value $v^{-1}(\partial v/\partial T)_p=3\alpha=1.2\times10^{-4}/°C$ gives the value of Γ for AP as $\Gamma_{AP}=0.746$. Because shock velocities of interest are in the 6 mm/μsec region, and because of uncertainties in the thermodynamic data, we decided to base our EOS for AP on the U=2.90+1.59u Hugoniot curve and the value $\Gamma_{AP}=0.75$. We also assumed C_v to be constant, and used these values of Γ and $v^{-1}(\partial v/\partial T)_p$ with T=298K in the thermodynamic identity

$$C_p = C_v(1+\frac{T\Gamma}{v}\frac{\partial v}{\partial T_p}) \tag{2.3.38}$$

to calculate the value for C_v as $(C_v)_{AP}=0.302$ cal/g k.

Having assigned these values of the shock and thermodynamic parameters to AP, the combination of Eqs. (2.3.5), (2.1.14), and (2.3.19) allows us to write the g function for AP as

$$g_{AP}(V) = 1.8333(\rho_0)_{AP}(\frac{a}{B})^2[1-b_1\frac{v_0}{\bar{V}}-b_2(\frac{v_o}{\bar{V}})^2] \quad for\ V\le 1 \tag{2.3.39}$$

with a=2.9 mm/μsec, B=1.59, $b_1=0.8436$, $b_2=0.1564$ and $\bar{V}=((1-B)v_0+Bv)$. Equation (2.3.2), with $\Gamma_{AP}=0.75$ and $g_{AP}(V)$ given by Eq. (2.3.39) can now be used to calculate the isentrope through the initial state (v_0,p=0). For notational convenience, the subscript AP will be mostly omitted from now on.

2.3.2.1. The Isentrope Through the Initial State

The differential equation for the isentropes is readily derived by equating the expression de=-pdv, obtained from the first laws of theormodynamics, and the expression for de obtained by differentiating Eq. (2.3.2):

$$vdp+(\Gamma+1)pdv = -\Gamma\frac{dg}{dv}dv\ . \tag{2.3.40}$$

Formally integrating Eq. (2.3.40) from an initial condition ($v=v_i$, $p=p_i$) gives the equation

$$pv^{\Gamma+1} = p_i(v_i)^{\Gamma+1}+\Gamma(v^{\Gamma}g(v)-v_i^{\Gamma}g(v_i))+\Gamma^2 I_i \tag{2.3.41}$$

with $I_i = \int_{v_i}^{v} v^{\Gamma-1}g(v)dv$, which gives the equation for the isentrope passing through the initial state ($v_i=v_0$, $p_i=0$) as

$$pv^{\Gamma+1} = \Gamma v^{\Gamma}g(v)+\Gamma^2 I. \tag{2.3.41.1}$$

with $I_0 = \int_{v_0}^{v} v^{\Gamma-1}g(v)dv$, because $g(v_0)=0$. For convenience in evaluating I_0, we set

$$I_0 = a_1 I_1 - a_2 v_0 I_2 - a_3 v_0^2 I_3 \tag{2.3.42}$$

with $a_1=1.8333(a/B)^2$, $a_2=1.5466(a/B)^2$, $a_3=0.2867(a/B)^2$ and

$$I_1 = \int_{v_0}^{v} v^{-\frac{1}{4}} dv \ , \ I_2 = \int_{v_0}^{v} v^{-\frac{1}{4}} \bar{V}^{-1} dv \ , \ I_3 = \int_{v_0}^{v} v^{-\frac{1}{4}} \bar{V}^{-2} dv \ .$$

Our construction of the isentrope through the initial state then proceeds as follows.

We first perform the itegration in I_1 to obtain the equation

$$I_1 = \frac{4}{3}(v_0)^{3/4} \ (V^{3/4}-1) \tag{2.3.43}$$

with $V=v_0/v$, and change variables, by setting $v=X^4$ and $\bar{V}=B(X^4-B_1)$ with $B_1=(B-1)v_0/B$. With this change of variables, I_2 and I_3 become

$$I_2 = \frac{4}{B} \int_{X_0}^{X} \frac{X^2 dX}{X^4-B_1} \tag{2.3.44}$$

and

$$I_3 = \frac{4}{B^2} \int_{X_0}^{X} \frac{X^2 dX}{(X^4-B_1)^2} \ . \tag{2.3.45}$$

We then use the identities

$$-d\frac{1}{X(X^4-B_1)} = \frac{dX}{X^2(X^4-B_1)} + \frac{4X^2 dX}{(X^4-B_1)^2} \tag{2.3.46}$$

and

$$-\frac{1}{X^2(X^4-B_1)} = \frac{1}{B_1}\left[\frac{1}{X^2} - \frac{X^2}{(X^4-B_1)}\right] \tag{2.3.47}$$

to transform the integral I_3 in two steps, the first by parts and the second by using partial fractions, into the equation

$$I_3 = \frac{1}{(B-1)v_0^{5/4}}\left[\frac{V^{3/4}}{(BV-(B-1))} - 1\right] - \frac{I_2}{4(B-1)v_0} \ . \tag{2.3.45)'}$$

At this stage, it is convenient to rewrite the equation for I_0 as

$$I_0 = \frac{4}{3}a_1(v_0)^{3/4}(V^{3/4}-1) + \frac{a_3(v_0)^{3/4}}{B-1}\left[\frac{V^{3/4}}{BV-(B-1)} - 1\right] + \left(\frac{a_3}{4(B-1)} - a_2\right)v_0 I_2 \ . \tag{2.3.48}$$

We finally use partial fractions to perform the integration in I_2 and obtain the following equation:

$$I_2 = B^{-1}\left(\frac{B}{(B-1)v_0}\right)^{1/4}\left\{\ln\frac{V^{\frac{1}{4}}-\left(\frac{B-1}{B}\right)^{\frac{1}{4}}}{V^{\frac{1}{4}}+\left(\frac{B-1}{B}\right)^{\frac{1}{4}}} + \ln\frac{1+\left(\frac{B-1}{B}\right)^{\frac{1}{4}}}{1-\left(\frac{B-1}{B}\right)^{\frac{1}{4}}} + 2\left(\tan^{-1}\left(\frac{BV}{B-1}\right)^{\frac{1}{4}} - \tan^{-1}\left(\frac{B}{B-1}\right)^{\frac{1}{4}}\right)\right. \tag{2.3.44)'}$$

which together with Eq. (2.3.45)′ defines the integral I_3 as a function of the reduced volume

$V=v/v_0$.

Equation (2.3.39) and Eqs. (2.3.44)′ and (2.3.48) were used to calculate values of $g_{AP}(V)$, I_2 and $I_0(V)$ over the reduced volume range $0.62 \le V \le 1$, and then Eq. (2.3.41.1) was used with these values of $g_{AP}(V)$, $I_0(V)$, and $\Gamma_{AP}=0.75$ to calculate values of the pressure p_s on the isentrope over the same volume range. These values of $g_{AP}(V)$, $I_0(V)$, and p_s are given in Table 2.2, as well as the values of the temperature along the isentrope calculated from the equation

$$T = T_i\left(\frac{v_i}{v}\right)^{0.75} \tag{2.3.49}$$

with $v_i=v_0$ and $T_i=T_0$.

To complete this series of EOS calculations for AP, we calculated values of the pressure p_H and temperature T_H along the Hugoniot in the (V-p) plane over the same reduced volume range, $0.62 \le V \le 1$. These values of p_H and T_H are also given in Table 2.2. The values of p_H were calculated from Eq. (2.3.19) with $v_0=0.513$ cm^3/g, a=2.90 mm/μsec and B=1.95, and the values of T_H were calculated by substituting the corresponding values of T_s, p_s, and p_H into the equation

$$T_H = T_s + V\frac{p_H - p_s}{\rho_0 \Gamma C_v} \tag{2.3.50}$$

with $\rho_0=1.95$ g/cm^3, $\Gamma_{AP}=0.75$ and $(C_v)_{AP}=1.264\times10^{-2}$ kbar cm^3/g K.

Examination of the values of T_H in Table 2.2 leads us to question this treatment of AP because we do not expect the shock temperature to reach such high values in the 300-400 kbar region. The reason for these high temperatures is clearly seen by considering Eq. (2.3.50). As V decreases and (p_H-p_s) increases, the difference (T_H-T_s) becomes magnified because C_v and Γ are assumed to be constant and $\Gamma<1$. We suggest that a task to investigate the validity of these assumptions be made a task in any additional work that may be performed on explosive compositions containing AP.

2.3.2.2. The Family of Isentropes Intersecting the Hugoniot Curve.

Because of our assumption about the behavior of reacting AP behind a shock, we must have a method for calculating the relationship between the pressure and volume along isentropes that intersect the shock. An equation providing this relationship along the isentrope passing through a point (v_H, p_H, T_H) on the Hugoniot is readily obtained by arranging Eq. (3.2.50), with $T_s=T_H(v_H/v_0)^{0.75}$ as

$$p_s = p_H - \rho_0 \frac{\Gamma C_v T_H}{V}\left(1-\left(\frac{V_H}{V}\right)^{0.75}\right) \tag{2.3.50}'$$

with $V_H=v_H/v_0$.

Table 2.2. Values of $v_0^{AP}g_{AP}(V)$, $I_0/(v_0)_{AP}^{3/4}$ the pressure p_s and temperature T_s along the $(v_0^{AP}, p=0)$ isentrope; the shock pressure p_H and the shock temperature T_H for different values of the reduced volume $V=v/v_0$.

V	$-v_0^{AP} g_{AP}(v)$ $(mm/\mu sec)_2$	$I_0/(v_0)^{3/4}_{AP}$ $(mm/\mu sec)^2$	p_s kbar	T_s K	p_H kbar	T_H K
1.0	0.000	0.000	0.0	298.0	0.0	298.0
0.95	0.616	0.016	9.68	309.7	9.68	309.7
0.90	1.368	0.066	23.09	322.5	23.19	327.1
0.85	2.302	0.160	41.95	336.6	42.42	358.2
0.80	3.496	0.311	68.95	352.3	70.52	420.2
0.75	5.068	0.537	108.57	369.8	112.94	547.1
0.70	7.226	0.866	168.68	389.4	179.86	812.9
0.65	10.351	1.347	264.30	411.6	291.82	1379.6
0.62	12.990	1.736	350.34	426.5	397.80	2018.8

2.3.3. A Method to Extend Equations of State Based On Shock Wave Data

We describe here another set of E,P,V and T,P,V equations of state of AP, which differ from those derived in Section 2.3.2 in the following ways. With respect to the E,P,V equation of state, the two are identical for the region $V \leq V_0$; in this section, we extend the equation of state to the region $V>V_0$, which was not done in Section 2.3.2. The T,P,V equations of state are different in that c_v=constant is assumed in Section 2.3.2, whereas in this section, we use, instead, the experimental coefficient of volume expansion and specific heat at constant pressure along the 1 bar isobar. The derivations provided below closely follow the earlier theoretical results of Enig.[9]

Enig[9] used the following Mie-Gruneisen form of the E,P,V equation of state, which we now apply to ammonium perchlorate:

$$P-P_r(V)=(\gamma/V)[E-E_r(V)], \tag{2.3.51}$$

where P,V, and E are, respectively, the pressure, specific volume, and specific internal energy, γ is the Gruneisen coefficient (assumed to be a constant for all P and V), and subscript r refers to the reference state to be specified below. It should be noted that Eq.(2.3.51) is a first-order Taylor expansion in the neighborhood of the reference curve,[1] and

$$\gamma=V(\partial P/\partial E)_V=\text{constant}. \tag{2.3.52}$$

In order to evaluate γ, we note that the definition of the sound speed c,

$$c^2=V^2[P(\partial P/\partial E)_V-(\partial P/\partial V)_E], \tag{2.3.53}$$

may be rewritten as

$$c^2/V^2=[P+(\partial E/\partial V)_p](\partial P/\partial E)_V$$

$$=(c_p/\beta V)(\partial P/\partial E)_V, \tag{2.3.54}$$

where

$$\beta=(1/V)(\partial V/\partial T)_P \tag{2.3.55}$$

and c_p are, respectively, the coefficient of thermal expansion and specific heat at constant pressure. From Eqs. (2.3.52) and (2.3.54), it follows that

$$\gamma=\beta c^2/c_p, \tag{2.3.56}$$

where β, c, and c_P may be chosen at the initial state (P_o,V_o,E_o,T_o), i.e.,

$$\gamma=\gamma_o=\beta_o c_{o2}/c_{p,o}, \tag{2.3.57}$$

and the subscript o refers to the initial state P_o=1 bar, T_o=298°K.

Thus far, the reference state has not been specified. Usually, for $V\leq V_o$, the Hugoniot originating at the initial state E_o,P_o,V_o is chosen as the reference state; we also shall do that. For the usual application of an E,P,V equation at high pressures as encountered, e.g., in the shocking of a metal, the thermodynamic states are limited to $V<V_o$. However, when the shocked state is subsequently expanded isentropically by a rarefaction wave originating at a free surface, the end state may have $V>V_o$. If $P_r(V)$ and $E_r(V)$ refer to the Hugoniot, V is not defined for $V>V_o$. The usual way this dilemma is treated is formally to extend the P,V Hugoniot relationship to $V>V_o$, i.e., into the "rarefaction shock" region. It is argued that the second-order tangency of the Hugoniot and the isentrope at (P_o,V_o,E_o) justifies this extrapolation if the volume increase in the expanded state, produced by the irreversible shock heating, is small.[13] This argument may be acceptable for the calculation of material motion, but probably would lead to large errors in the calculation of the temperature of the shocked state. It will be shown below that the temperature of the shocked state is a sensitive function of the T,V variation along $P=P_o$ and the slope of the P,V isentropes at $P=P_o$. For this reason, we shall use the isobar $P=P_o$ as the pressure reference state P_r and $E_r(V)=E(P_o,V)$ as the internal energy reference state.

2.3.3.1. Region 1: $V \geq V_o$

In the low-pressure region $V\geq V_o$, Enig defined[9]

$$P_r(V)=P_o \tag{2.3.58}$$

$$E_r(V)=E(P_o,V). \tag{2.3.59}$$

By integration of the thermodynamic identity

$$(\partial E/\partial V)_P=c_P/\beta V-P \tag{2.3.60}$$

along $P=P_o$, we find

$$E(P_o,V)=E_o+\int_{Vo}^{V}[c_p/\beta V'-P_o]dV', \tag{2.3.61}$$

where $E_o=E(P_o,V_o)$, the specific internal energy at the initial state, is an arbitrary constant that can be set equal to zero if desired. If $c_p=c_{p,o}$ and $\beta=\beta_o$ on $P=P_o$, Eqs. (2.3.55) and (2.3.61) yield

$$T(P_o,V)=T_o+(1/\beta_o)\ell n(V/V_o) \tag{2.3.62}$$

$$E_r(V)=E(P_o,V)=E_o+(c_{p,o}/\beta_o)\ell n(V/V_o)-P_o(V-V_o). \quad (2.3.63)$$

It should be noted that though all terms involving P_o are negligible, they will be kept in order that all thermodynamic relationships to be derived are formally exact. Equation (2.3.51) becomes

$$E=E_o-P_o(V-V_o)+(c_{p,o}/\beta_o)\ell n(V/V_o)+(P-P_o)V/\gamma \quad \text{for } V\geq V_o. \quad (2.3.64)$$

Enig[14] has shown that the thermodynamic identity

$$[P+(\partial E/\partial V)_P](\partial T/\partial P)_V-(\partial E/\partial P)_V(\partial T/\partial V)_P=T \quad (2.3.65)$$

yields the characteristic equations

$$dP/dV+[P+(\partial E/\partial V)_P]/(\partial E/\partial P)_V=0 \quad (2.3.66)$$

$$dT/dV+T/(\partial E/\partial P)_V=0, \quad (2.3.67)$$

which with an E,P,V equation of state and a nonisentropic initial curve along which the temperature is prescribed, e.g., Eq. (2.3.62), leads to a T,P,V equation of state as described below.

The solution of Eq. (2.3.66) yields the isentropes

$$C_1=[(P-P_o)V+c_{p,o}/\beta_o]V^\gamma, \quad (2.3.68)$$

where the constant of integration C_1 is different for each isentrope, i.e., C_1 varies with the entropy S. The solution of Eq. (2.3.67) along an isentrope is

$$C_2=TV^\gamma, \quad (2.3.69)$$

where C_2, the constant of integration, varies with S. Substitutions of $P=P_o$ into Eq. (2.3.68) and Eq. (2.3.62) into Eq. (2.3.69) yield, respectively, C_1 and C_2 as functions of the parameter V (the specific volume along $P=P_o$):

$$C_1=c_{p,o}V^\gamma/\beta_o \quad \text{on } P=P_o \quad (2.3.70)$$

$$C_2=[T_o+(1/\beta_o)\ell n(V/V_o)]V^\gamma \quad \text{on } P=P_o. \quad (2.3.71)$$

For convenience, replace V in the above equations by z. Equations (2.3.68) and (2.3.69) are now

$$[(P-P_o)V+c_{p,o}/\beta_o]V^\gamma=c_{p,o}z^\gamma/\beta_o \quad (2.3.72)$$

$$TV^\gamma=[T_o+(1/\beta_o)\ell n(z/V_o)]z^\gamma \quad (2.3.73)$$

Elimination of the parameter z between Eqs. (2.3.72) and (2.3.73) yields the P,V,T equation of state:

$$T(P,V)=x[T_o+(1/\beta_o)\ell n(x^{1/\gamma}V/V_o)], \quad (2.3.74)$$

where

$$x(P,V)=1+\beta_o(P-P_o)V/c_{p,o}. \quad (2.3.75)$$

In particular, on $V=V_o$:

$$T(P,V_o)=T_o[1+\beta_o(P-P_o)V_o/c_{p,o}]\{1+(1/\gamma\beta_oT_o)\ell n[1+\beta_o(P-P_o)V_o/c_{p,o}]\} \quad (2.3.76)$$

2.3.3.2. Region 2: $V<V_o$

For $V<V_o$, Enig[9] chose the Hugoniot pressure $P_H(V)$ as the reference pressure $P_r(V)$, where the origin of the Hugoniot is the initial state (P_o,V_o,E_o). Thus, Eq. (2.3.51) is now

$$P=P_H(V)+(\gamma/V)[E-E_H(V)]. \quad (2.3.77)$$

Substitution of Eq. (2.3.77) into the isentropic relationship

$$dE+PdV=0 \quad (2.3.78)$$

and use of the shock condition

$$E_H-E_o=(P_H+P_o)(V_o-V)/2, \quad (2.3.79)$$

yields

$$dE/dV+\gamma E/V=\gamma[E_o+\tfrac{1}{2}P_o(V_o-V)]/V+\tfrac{1}{2}\gamma P_H(V_o-V)/V-P_H, \quad (2.3.80)$$

whose general integral is

$$C_3=(V/V_o)^\gamma[E-E_o-\tfrac{1}{2}P_oV_o+\tfrac{1}{2}\gamma P_oV/(\gamma+1)]+E_o+\tfrac{1}{2}P_oV_o/(\gamma+1)+I(V), \quad (2.3.81)$$

where

$$I(V)=\tfrac{1}{2}V_o^{-\gamma}\int_{Vo}^{V}v^\gamma(2+\gamma-\gamma V_o/v)P_H(v)dv \quad (2.3.82)$$

and C_3 is the constant of integration defining the isentrope in the E,V plane. In terms of the as yet unknown Hugoniot $P_H(V)$, the isentropes in the P,V plane are obtained by substitution of E from Eq. (2.3.77) into Eq. (2.3.81):

$$C_3=(\frac{V}{V_o})^\gamma[(P-P_H)\frac{V}{\gamma}+\tfrac{1}{2}(P_H+P_o)(V_o-V)-\tfrac{1}{2}P_oV_o+\tfrac{1}{2}\gamma\frac{P_oV}{\gamma+1}]+E_o+\tfrac{1}{2}\frac{P_oV_o}{\gamma+1}+I(V). \quad (2.3.83)$$

To this point, the analysis for Region 2 is general in terms of an as yet nonprescribed Hugoniot curve $P_H(V)$. For simplicity of analysis, Enig[9] limited himself to those unreacted explosives (as well as metals) that satisfy the experimental shock condition

$$U=c_o+au, \quad (2.3.84)$$

where U and u are, respectively, the shock velocity and particle velocity, and c_o and a are empirical constants.[15,12] In theory, the c_o of Eq. (2.3.84) should be the same as the initial sound speed of Eq. (2.3.57), but in practice it is not because Eq. (2.3.84) generally does not hold as $u\to 0$. It follows from the Rankine-Hugoniot conditions that

$$P_H(V)=P_o+c_o^2(V_o-V)/[V_o-a(V_o-V)]^2. \quad (2.3.85)$$

Substitution of Eq. (2.3.85) into Eq. (2.3.82) gives

$$I(V)=\tfrac{1}{2}P_oV_o[(\gamma+2)R^{\gamma+1}/(\gamma+1)-R^{\gamma}-(\gamma+1)^{-1}]+c_o^2A^{\gamma+1}(\gamma+1)(a-1)^{-2}J(V), \quad (2.3.86)$$

where

$$R=V/V_o \quad (2.3.87)$$

$$J(V)=\int_A^{B(V)}t^{-\gamma}(mt-1+n/t)(1-t)^{-2}dt \quad (2.3.88)$$

$$m=\tfrac{1}{2}\gamma a/[(a-1)(\gamma+1)] \quad (2.3.89)$$

$$n=\tfrac{1}{2}(\gamma+2)(a-1)/(\gamma+1)a \quad (2.3.90)$$

$$A=1-a^{-1}<1 \quad (2.3.91)$$

$$B(V)=AV_o/V\le 1, \quad (2.3.92)$$

and the transformation $t=(1-a^{-1})V_o/v$ has been used. It should be noted $B(V)\le 1$, where the equality holds only as $V/V_o\to 1-a^{-1}$ as $P_H\to\infty$ in Eq. (2.3.85).

Using partial fractions, Eq. (2.3.88) becomes

$$J(V)=\int_A^{B(V)}t^{-\gamma}[A_1t^{-1}+A_2(1-t)^{-1}+A_3(1-t)^{-2}]dt, \quad (2.3.93)$$

where

$$A_1=n,\ A_2=n-m,\ A_3=m+n-1. \quad (2.3.94)$$

But

$$\int_A^{B(V)}t^{-\gamma}(1-t)^{-2}dt=B^{1-\gamma}(1-B)^{-1}-A^{1-\gamma}(1-A)^{-1}+\gamma\int_A^{B(V)}t^{-\gamma}(1-t)^{-1}dt, \quad (2.3.95)$$

which when substituted into Eq. (2.3.93) yields

$$J(V)=[A_1/\gamma-AA_3/(1-A)]A^{-\gamma}-[A_1/\gamma-BA_3/(1-B)]B^{-\gamma}+(A_2+\gamma A_3)\int_A^{B(V)}t^{-\gamma}(1-t)^{-1}dt. \quad (2.3.96)$$

By Eqs. (2.3.83), (2.3.86), and (2.3.96), the evaluation of the constant C_3, which characterizes an isentrope, entails the evaluation of the integral in Eq. (2.3.96). To evaluate the integral, we note that

$$\begin{aligned}\int_A^{B(V)}t^{-\gamma}(1-t)^{-1}dt&=\int_A^{B(V)}t^{N-\gamma}dt/[t^N(1-t)]=\int_A^{B(V)}t^{N-\gamma}dt\Sigma t^{-k}+\int_A^{B(V)}t^{N-\gamma}(1-t)^{-1}dt\\&=\int_A^{B(V)}t^{N-\gamma}(1-t)^{-1}dt+\Sigma(B^{N-k-\gamma+1}-A^{N-k-\gamma+1})/(N-k-\gamma+1)\\&=\int_A^{B(V)}t^{s-1}(1-t)^{-1}dt+\Sigma(B^{s-k}-A^{s-k})/(s-k), \quad (2.3.97)\end{aligned}$$

where the summation is taken from k=1 to k=N, N is the smallest non-negative integer greater than $\gamma-1$,

$$s=N-\gamma+1>0, \tag{2.3.98}$$

and the integral[16]

$$\int_A^{B(V)} t^{s-1}(1-t)^{-1}dt=s^{-1}B^s{}_2F_1(1,s;1+s;B)-s^{-1}A^s{}_2F_1(1,s;1+s;A), \tag{2.3.99}$$

is given in terms of Gauss's hypergeometric series.[17] Note that if N=0, the summation term on the right-hand side of Eq. (2.3.97) is set equal to zero. The exact derivation of the P,V isentrope characterized by some value of C_3 (a function of the entropy) is complete.

In order to avoid the need to evaluate Gauss's hypergeometric series, the integral in Eq. (2.3.96) can be accurately approximated by fitting $(1-t)^{-1}$ by a polynomial in t over the range $0<1-a^{-1}=A\le t\le B(V)=AV_o/V<1$ and carrying out the resulting simple integration. A *single* polynomial fit can be made to work for almost all explosives over a single interval $A_{min}\le t\le B_{max}$, where $A_{min}\simeq 0.2$ and $B_{max}\simeq 0.9$:

$$(1-t)^{-1} = \Sigma_{n=o}^{7}\, a_n t^n,$$

where $a_0 = 13.29242189$, $a_1 = 247.2782554$, $a_2 = 1745.422711$, $a_3 = 6618.403805$, $a_4 = 14505.10394$, $a_5 = 18455.64985$, $a_6 = -12662.06958$, and $a_7 = 3633.143062$.

The solution of Eq. (2.3.67) along an isentrope is

$$C_4=TV^\gamma, \tag{2.3.100}$$

where the subscript 4 is used in this region to distinguish the isentrope from that in Region 1 given by Eq. (2.3.69). Substitution of Eq. (2.3.76) into Eq. (2.3.100) yields C_4 as a function of the parameter P on the non-characteristic (non-isentropic) line $V=V_o$; then, for convenience, P is replaced by the new parameter y. By Eq. (2.3.100) the temperature along the isentrope is now given by

$$TV^\gamma=T_oV_o^\gamma[1+\beta_o(y-P_o)V_o/c_{p,o}]\{1+(1/\gamma\beta_oT_o)\ell n[1+\beta_o(y-P_o)V_o/c_{p,o}]\}. \tag{2.3.101}$$

Substituting $V=V_o$ into Eq. (2.3.83) yields

$$C_3=E_o+(P-P_o)V_o/\gamma \quad \text{on } V=V_o. \tag{2.3.102}$$

Replacing P by y in Eq. (2.3.102) and substituting the result into Eq. (2.3.83) gives the P,V isentrope:

$$y=P_o+\frac{\gamma}{V_o}\left\{\left(\frac{V}{V_o}\right)^\gamma\left[(P-P_H)\frac{V}{\gamma}+\tfrac{1}{2}(P_H+P_o)(V_o-V)-\tfrac{1}{2}P_oV_o+\tfrac{1}{2}\gamma P_o\frac{V}{\gamma+1}\right]+\tfrac{1}{2}\frac{P_oV_o}{\gamma+1}+I(V)\right\}. \tag{2.3.103}$$

Equations (2.3.101) and (2.3.103) define the T,P,V equation of state for Region 2 in terms of the parameter y. Thus, for known P and V, y is found from Eq. (2.3.103) (remembering that P_H is given by Eq. (2.3.85)) and then substituted into Eq. (2.3.101) to yield T.

2.3.3.3. Connecting the Isentropes of Regions 1 and 2 at $V=V_o$:

The P,V isentropes in Regions 1 and 2, which are given, respectively, by Eqs. (2.3.68) and (2.3.83), meet at $V=V_o$. Substituting $V=V_o$ in Eqs. (2.3.68) and (2.3.73) and eliminating P between the resulting equations give

$$C_1=[\gamma(C_3-E_o)+c_{p,o}/\beta_o]V_o^{\gamma}. \qquad (2.3.103.1)$$

2.3.4. A Thermodynamic Model For Al_2O_3.

An examination of the shock wave data for corundum[15], α-Al_2O_3, with a density of $(\rho_0)_1=3.98$ g/cm^3, and our shock pressure range of interest led us to conclude that an adequate thermodynamic treatment of α-Al_2O_3 and γ-Al_2O_3 can be based on the assumption that the Hugoniot curves are straight lines. In this case, the equations for the pressure and energy along these Hugoniot curves can be written as

$$p = (\rho_0 c_0)_i^2 (v_0 - v)_i \ , \ i=1 \ or \ 2 \ , \qquad (2.3.104)$$

and

$$e_i-(e_0)_i = \frac{(\rho_0 c_0)_i^2}{2}(v_0-v)_i^2 \ , \ i=1 \ or \ 2 \ , \qquad (2.3.105)$$

where $(c_0)_i$ denotes the constant shock velocities, $(e_0)_i = (\Delta h_f^0)^i_{Al_2O_3}$, and the Hugoniot curves are also isentropes because Eq. (2.3.105) satisfy the equation $de_i=-pdv_i$. The combination of Eqs. (2.3.104), (2.3.105) and the e=e(p,v) EOS given by Eq. (2.1.16) gives the following equations for the $g_i(V)$ functions for Al_2O_3:

$$g_i(V) = \rho_0^i \frac{(c_0)_i^2}{2}\left(1-\frac{2(\Gamma+1)V}{\Gamma}+\frac{(\Gamma+2)V^2}{\Gamma}\right)_i \ for \ V\le 1 \ , \ i=1 \ or \ 2 \ . \qquad (2.3.106)$$

To proceed with our thermodynamic model, we assumed that α-Al_2O_3 and γ-Al_2O_3 have constant values of Γ and C_v. With literature values of $(C_p)_1=0.775\times10^{-2}$ kbar cm^3/g K, $((\partial v/\partial T)_p)_1=5.108\times10^{-6}$ kbar cm^3/g K for α-Al_2O_3, and a value $(c_0)_1=9.64$ mm/μsec suggested by the shock-wave data, Eqs. (2.3.37) and (2.3.38) give the values $\Gamma_1=2.44$ and $(C_v)_1=0.764\times10^{-2}$ kbar cm^3/g K, for α-Al_2O_3.

Now with the limited amount of thermodyanamic data available, we have to formulate a procedure for deciding whether α-Al_2O_3 or γ-Al_2O_3 is present in our reacting explosive compositions containing Al. We base this formulation on the fact that α-Al_2O_3 is the most stable form of Al_2O_3 in the standard states (p=0, T=298, $v=(v_0)_i$), and on the premise that the Hugoniot curves of α-Al_2O_3 and γ-Al_2O_3 intersect at a point (v_j, p_j) in the (v,p) plane. Then, Al_2O_3 will be assumed to be in the α-form when $p<p_j$, but in the γ-form when $p>p_j$. Our justification, for this assumption as well as our procedure for evaluating unknown thermodynamic parameters for γ-Al_2O_3 is based on the following calculations of the Gibbs free energies G_1 and G_2 for α-Al_2O_3 and γ-Al_2O_3 , respectively.

Our free energy calculations are based on the thermodynamic data for α-Al_2O_3 and γ-Al_2O_3, which are listed in the 66th Edition of the Handbook of Chemistry and Physics (HCP)[18]. The values given for the heat of formation and entropy for α-Al_2O_3 in the standard state (p=1 atm, T=298.15 K) are $(\Delta H_f^0)_1=-400.5$ kcal/mol and $S_1^0=12.17$ cal/deg mol. In constrast to α-Al_2O_3 , a range of values of $(\rho_0)_2$ and $(\Delta H_f^0)_2$ are given for γ-Al_2O_3, and no value for S_2^0 is given. To be

more specific, as γ-Al_2O_3 changes from its amorphous to crystalline form in the standard state, $(\rho_0)_2$ varies from 3.5-3.9 g/cm^3 and $(\Delta H_f^0)_2$ varies from -390 to 395 kcal/mol. Additional background information for our thermodynamic model of Al_2O_3 was the following experimental observation from a paper by A.J. Brock and M.J. Pryor,[19]: the only oxidation product formed by pure Al subjected to low pressures of O_2 in the 300-425°C temperature range is amorphous γ-Al_2O_3. This observation suggests that the γ-Al_2O_3 formed during the detonation process will be in a somewhat amorphous state; it allows us to make an estimate of the standard entropy S_2^0 of this amorphous γ-Al_2O_3.

Our estimate of S_2^0 is based on the assumptions that α-Al_2O_3 and amorphous γ-Al_2O_3 have the same values of C_p, $(C_p)_1=(C_p)_2$, and that $G_1=G_2$ at 300°C. In this case, the equation

$$(\Delta H_f^0)_1 - TS_1^0 = (\Delta H_f^0)_2 - TS_2^0 \qquad (2.3.107)$$

with T=573 K, the values for $(\Delta H_f^0)_1$ and S_1^0 given above, and a value of $(\Delta H_f^0)_2$=-392 kcal/mol gives a value for the standard entropy of amorphous γ-Al_2O_3 of S_2^0=27.00 cal/deg mol.

At this stage in our treatment of Al_2O_3, we have two adjustable parameters, p_j and $(\rho_0)_2$, whose values must be specified before this model can be utilized. Because values for these parameters are not known at this time, we first present a procedure for completing this model when p_j and $(\rho_0)_2$ are prescribed, and then exemplify it by using particular values for p_j and $(\rho_0)_2$.

Our procedure for closing our thermodynamic treatment of Al_2O_3, when p_j and $(\rho_0)_2$ are prescribed, is as follows. First, use the value of p_j in Eq. (2.3.104) with i=1 to determine the value of v_j, and use this value of v_j in the following equation with i=1,

$$(T_j)_i = T_0\left(\frac{(v_0)_i}{v_j}\right)^{\Gamma_i}, \qquad (2.3.108)$$

to calculate the value of $(T_j)_1$, at (v_j, p_j). Next, use the condition $G_1=G_2$ at the point (v_j, p_j) to calculate $(T_j)_2$, and use Eq. (2.3.108) with j=2 to calculate the corresponding value of Γ_2. Because $(c_0)_2$ is known from Eq. (2.3.104) when p_j and $(v_0)_2$ are specified, and $(C_p)_1=(C_p)_2$ by hypothesis, Eq. (2.3.37) can be used to calculate the corresponding value of $((\partial v/\partial T)_p)_2$ for γ-Al_2O_3. We will now carry out this procedure in detail for the case when p_j=100 kbar and $(\rho_0)_2$=3.52 g/cm^3.

Thus, we first set p_j=100 kbar in Eq. (2.3.104) with $(\rho_0 c_0^2)_1=3.698\times10^3$ kbar to obtain the corresponding value of v_j=0.2445 cm^3/g. Equation (2.3.108) with i=1 and Γ_1=2.44 then gives a value of $(T_j)_1$=318.6 K and Eq. (2.3.104) with i=2 and $(v_0)_2$=0.2841 cm^3/g gives the value of $(c_0)_2$=4.515 mm/μsec. We next write the equations for G_1 and G_2 at (v_j, p_j) as

$$G_1 = (\Delta H_f^0)_1 + \frac{p_j}{2}((v_0)_1+v_j)-(T_j)_1 S_1^0 \qquad (2.3.109.1)$$

and use the equation obtained by setting $G_1=G_2$ to calculate a value of $(T_j)_2$=613 K, which is used in Eq. (2.3.108) with i=2 to calculate a value of Γ_2=4.80. Because the value of $(T_j)_2$=340°C lies

$$G_2 = (\Delta H_f^0)_2 + \frac{p_j}{2}((v_0)_2+v_j)-(T_j)_2 S_2^0 \qquad (2.3.109.2)$$

towards the bottom of the temperature range reported for the formation of amorphous γ-Al_2O_3 at low pressures, it is reasonable to choose p_j=100 kbar and $(\rho_0)_2$=3.52 cm^3/g as the values for these parameters in a first-generation thermodynamic model for Al_2O_3 developed in Task 1. The calculated value of Γ_2=4.80 leads to the conclusion that in this treatment of Al_2O_3 the thermal coefficient of amorphous γ-Al_2O_3, $((\partial v/\partial T)_p)_2$, is ten times greater than the thermal coefficient of α-Al_2O_3, $((\partial v/\partial T)_p)_1$.

In any future work to be performed on explosive compositions contains Al, the method presented in the previous section should be used to extend these EOS for α-Al_2O_3 and amorphous γ-Al_2O_3 beyond the volume ranges spanned by their Hugoniot curves. Melting of Al_2O_3 should also be considered.

2.3.5. Polytropic Equations of State for the Detonation Products

The limitations of the polytropic EOS led to the development and implementation of more realistic EOS for detonation products[20,21]. More basic EOS for detonation products, based on the work of J.D. Weeks, D. Chandler, and H.C. Anderson[22] have been developed by F.H. Ree[23] and W.B. Brown[24] , and for detonation products containing Al by H.D. Jones and F.J. Zerilli[25] . These EOS address both the spherically averaged and multipole components of the temperature-dependent pair potential between the molecular species. Use of these EOS was considered, but we decided that there was insufficient time to adopt them in Phase I. For this reason, the polytropic EOS was considered to be adequate for our detonation modelling in Phase I. Consequently, the polytropic $E=E(p,v_f,m_{H2O})$ EOS of our AP/Al mixture has already been introduced in Section 2.1, and the polytropic $E=E(p,v_f,m_{H2O}, m_{CO2}, m_{C2H6})$ EOS for our $C_aH_bN_cO_d$/Al mixture can be seen in Eq. (2.2.20). These polytropic EOS extend those usually encountered in the literature by accounting quantitatively for the reactions of the detonation products with Al. The reaction coordinates used to describe the changing masses of some of the fluid constituents in the detonation products, however, were only included in the standard states term containing heats of formation as shown in Eq. (2.2.20).

Because these $E=E(p,v_f,m_{H2O})$ and $E=E(p,v_f,m_{H2O}, m_{CO2}, m_{C2H6})$ EOS are incomplete and provide no information about temperature, they are only adequate for treating the detonation process when the temperature need not be accounted for explicitly. Consequently, they are adequate for a detonation model when the solid components behind the shock are assumed to be constrained to their own isentropes, but not when a solid component such as Al_2O_3 is assumed to attain thermal equilibrium with the detonation products. Thus, it was necessary to construct a $T=T(p,V_f)$ EOS for detonation products to accomodate our assumption that $T_f=T_i$. This construction proceeds as follows.

2.3.5.1. A p=p(T,V) EOS of Detonation Products

To be consistent with the polytropic EOS introduced in previous sections, we write the complete $E=E(S_f,V_f, \xi_i)$ EOS for detonation products as

$$E = E_c(\xi_i)+E_1(S_f ,V_f), \; i=1,...m \; , \tag{2.3.110}$$

so that the extents of reaction ξ_i appear only in the standard state term $E_c(\xi_i)$. Now, because we are dealing with polytropic media only, it is convenient to omit the subscript f. In addition,

where it is convenient for our purpose, we will only consider one extent of reaction coordinate ξ.

In this case, the thermodynamic identities for T and p can be written as $T=\partial E_1/\partial S$ and $p=-\partial E_1/\partial V$, the EOS for T and p in terms of S can be written as T=T(S,V) and p=p(S,V), and S can be eliminated between these EOS to show that T=T(p,V). Thus, when $E=E(S,V,\xi)$ is written as $E=E_c(\xi)+E_1(S,V)$, the partial derivatives $(\partial T/\partial \xi)_{p,V}$, $(\partial T/\partial \xi)_{S,V}$, $(\partial p/\partial \xi)_{S,V}$, and $(\partial S/\partial \xi)_{T,V}$ are all zero, and it follows from the following identities for the chemical affinity A[26],

$$-A = (\frac{\partial E}{\partial \xi})_{S,V} = (\frac{\partial E}{\partial \xi})_{p,V} + (\frac{\partial E}{\partial p})_{\xi,V} (\frac{\partial \xi}{\partial p})_{S,V} , \tag{2.3.111}$$

that $-A=(\partial E/\partial \xi)_{p,V}$. Consequently, the ξ terms in $E_c(\xi)$ are only associated with the heats of formation of the species taking part in the reaction.

To proceed with our construction, we consider the case when E_1 is a separable function of S and V given by the equation

$$E_1 = V^{-n} E_1(S) , \tag{2.3.112}$$

where n is a constant parameter, and we differentiate this expression for E_1 to obtain equations for p and T. The identity for p gives the equation

$$\frac{pV}{n} = V^{-n} E_1(S) , \tag{2.3.113}$$

which together with Eq. (2.3.110) allows us to write the $E=E(p,V,\xi_i)$ EOS as

$$E = E_c(\xi_i) + \frac{pV}{n} \tag{2.3.114}$$

and identify the parameter n as $n=\gamma-1$. The identity for T gives the equation

$$T = V^{-n} dE_1/dS , \tag{2.3.115}$$

which leads to the following equation for C_v,

$$C_V = \frac{dE_1/dS}{d^2E_1/dS^2} . \tag{2.3.116}$$

We next combine Eq. (2.3.115) with the equation obtained by differentiating Eq. (2.3.113) partially with respect to T, to obtain the following equation:

$$(\frac{\partial p}{\partial T})_V = \frac{nC_v}{V} . \tag{2.3.117}$$

Because $(\partial S/\partial \xi)_{T,V}=0$, we can integrate the differentiated form obtained by combining the identity $dS=C_v dT/T+(\partial p/\partial T)_V dV$ and Eq. (2.3.117), to get

$$TV^n = \exp \int dS/C_v . \tag{2.3.118}$$

It follows from Eq. (2.3.116) that we cannot perform the integration in Eq. (2.3.118) until C_v is know as a function of S. We simply bypass this difficulty here by assuming that C_v is a constant. Then E_1 satisfies the equation $dE_1/dS=e^{S/C_v}$ which on integration yields the equation

$$E_1(S) = C_V T V^n + E_1^0 \ . \qquad (2.3.119)$$

Combining Eqs. (2.3.113) and (2.3.119) and setting n=γ-1 gives the p=p(T,V) EOS as

$$pV=(\gamma-1)C_V T + E_1^0/V^{\gamma-1} \qquad (2.3.120)$$

with E_1^0 a parameter to be determined.

We finally assume that our polytropic fluid has a mass m, set V=mv, and rewrite Eq. (2.3.120) in terms of specific quantities as

$$pv = (\gamma-1)c_v T + \hat{A}(\frac{\hat{v}}{v})^{\gamma-1} \qquad (2.3.120)'$$

with $c_v=C_V/m$ and a constant $\hat{A} = (\hat{p}\hat{v}-(\gamma-1)\hat{c}_v\hat{T})$. Equation (2.3.120)′ can be calibrated for detonation products by using known values of $\hat{p}$, $\hat{v}$, $\hat{T}$, *and* $\hat{c}_v$ at the CJ point to evaluate the constant $\hat{A}$.

2.4. Steady-State, Nonideal Detonation in an Explosive

2.4.1. Composition Containing Al

Our thermodynamic models for explosive compositions presented in Section 2.1 and 2.2 are both based on the tenet that a satisfactory treatment of nonideal detonation in an explosive composition containing aluminum (Al) must take account of the reaction of the explosive grains and Al particles in the reaction zone (RZ) neighboring the shock front. This tenet leads to two limiting cases of nonideal detonations, that propagate at constant velocity and consequently are supported by steady-state, reaction zones (SSRZ). In one of these cases, the time scale for the reaction of the Al with the explosive's products is much larger than the time scale for the decomposition of the explosive grains: all the Al passes through the SSRZ before it reacts with the product gases in the ensuing release wave. In the other case, the time scale for the reaction of Al with the explosive's products is significantly smaller than the time scale for the decomposition of the explosive grains: all the Al reacts in the SSRZ; the release wave can be modeled as an isentrope. Consequently, a constant-velocity, nonideal detonation will in general be represented by an intermediate case with Al reacting in both the SSRZ and the release wave, and rate functions for the decomposition of the explosive and the reactions of Al must be known before a thermo-hydrodynamic model for such a detonation can be used to calculate its properties. For these reasons, we performed two tasks to provide a more definitive background for nonideal detonation and thereby develop a better appreciation of its complications. In the first task, we developed a prototype model for SS, nonideal detonation, and in the second, a prototype model for burning explosive grains. The work performed on the first task will be presented in this section but the work performed on the second task will be presented in Appendix A.

To provide background for our treatment of SS, nonideal detonation, we first present the equations governing a SS detonation wave and then consider the relationship between its RZ length and corresponding reaction time.

2.4.2. Equations for a Steady-State Reaction Zone

Here, we will use the subscripts *x* and *p* to denote the explosive and its products, the subscript H to denote the shocked state, and either a superscript or a subscript 0 to denote the standard state of the explosive and the detonation products, i.e., at pressure p_0 and temperature T_0. Recalling that the Rankine-Hugoniot (RH) jump conditions are first integrals of the differential equations expressing the conservation laws when the flow has attained a SS, we write the equation governing our SSRZ as

$$\rho(D-u)=\rho_0 D, \tag{2.4.1}$$

$$p=\rho_0 D^2(1-v/v_0), \tag{2.4.2}$$

$$e-e_x^0=pv_0(1-v/v_0)/2, \tag{2.4.3}$$

with D and u used, respectively, to denote the detonation velocity and the particle velocity, and $p_0=0$. Eq. (2.4.1) expresses the conservation of mass, Eq. (2.4.2) expresses the conservation of mass and momentum, Eq. (2.4.3) expresses the conservation of mass, momentum, and energy, and the equations governing the shock at the front of the SSRZ are obtained by putting a subscript H on the variables ρ,u,p,v and *e* in Equations (2.4.1), (2.4.2), and (2.4.3).

To continue this treatment of our SSRZ, we introduce the sound speed c, define the adiabatic index k by the equation $c^2=kpv$, and recall that the SSRZ terminates at the Chapman-Jouquet (CJ) state where the flow become sonic. Using the subscript j to denote the CJ state, this sonic condition is expressed by the equations,

$$D-u_j=c_j, \tag{2.4.4}$$

The combination of the equations $\rho_j c_j=\rho_0 D$, $c_j^2=k_j p_j v_j$, and Eq. (2.4.2) written for the CJ state, then gives the well known equations for v,u,c, and ρ in the CJ state:

$$v_j/v_0=k_j/(k_j+1), \tag{2.4.5}$$

$$k_j u_j=c_j=Dk_j/(k_j+1), \tag{2.4.6}$$

$$p_j=\rho_0 D^2/(k_j+1). \tag{2.4.7}$$

We finally note that the relationship between D and the specific chemical energy *q* liberated by a particle passing through the SSRZ is derived by combining the e=e(p,v) equation of state for the detonation products with the following equation:

$$e_j-e_x^0=D^2/2(k_j+1)^2 \tag{2.4.8}$$

obtained by combining Eqs. (2.4.5) and (2.4.7) with Eq. (2.4.3) written for the CJ state. Having derived the RH jump conditions for SS flows, it is convenient to consider how RZ length and reaction time are related in a SS detonation.

2.4.3. The Relation Between Reaction Zone Length and Reaction Time in a Steady State Detonation Wave

Our purpose here is to derive equations that place upper and lower limits on the SSRZ length L when the detonation velocity D is known and the reaction time t_R has been estimated. We accordingly consider a one-dimensional, SS, ZND (Zeldovich, von Neumann, Doering) detonation wave. With our present notation, the equation for the RZ length can be written as

$$L = Dt_R - \int_0^{t_R} u\, dt\ , \tag{2.4.9}$$

where t denotes the time.

Because u drops linearly with p along the Rayleigh line representing the SSRZ, realistic equations for lower and upper limits of L can be obtained by setting, respectively, $u=u_H$ and $u=u_j$ in Eq. (2.4.9). To derive the equation for the lower limit L_-, we assume that shock velocity U,u_H Hugoniot curve for the explosive is linear, U=a+Bu, and use the value of $u_H=(D-a)/B$ in Eq. (2.4.9) to obtain the equation

$$L_- = D(1-(D-a)/DB)\, t_R. \tag{2.4.10}$$

To derive the equation for the upper limit L_+, we recall that $u_j=D/(k_j+1)$, where k denotes the adiabatic index $(\partial \ln p/\partial \ln v)_s$, and use this value for u_j to obtain the equation

$$L_+ = k_j D t_R/(k_j+1) \tag{2.4.11}$$

with the values of a=2.90 mm/μsec and B=1.59 for AP given by SFP[11] and the values of D=6.6 mm/μsec and k_j=3.45 for AP obtained from a TIGER code calculation. Equations (2.4.10) and (2.4.11) for AP become

$$L_- = 4.29\, t_R \tag{2.4.10}'$$

$$L_+ = 5.16\, t_R. \tag{2.4.11}'$$

Thus if t_R=0.5 μsec, the upper and lower limits for the length of the RZ in AP are, respectively, 2.58 mm and 2.14 mm.

It is now convenient to formulate our prototype model for SS nonideal detonation.

2.4.4. A Prototype Model for Nonideal Steady State Detonation

For convenience in formulating a prototype model for nonideal SS detonation, we again consider the $C_aH_bN_cO_dAl_f$ composition discussed in Section 2.2. We adopt the reaction scheme formulated for this composition, but for the sake of tractability, make more simplistic assumptions about the condensed components. We formulate the simplest treatment of detonation supported by (R.3) and (R.7) by assuming the following:

A.7 The explosive $X=C_aH_bN_cO_d$ is a polytropic explosive with the same index as the polytropic products.

A.8 Both Al and Al_2O_3 can be treated as incompressible solids, and the reaction between Al and H_2O produces only one form of Al_2O_3. With these assumptions, the e-relationship we previously developed for our $C_aH_bN_cO_dAl_f$ composition takes a much simpler form, and the subscript and superscript used to denote different forms of Al_2O_3 can be eliminated.

To be more definitive, we denote the specific volumes of X, Al and Al_2O_3 by v_x, $\bar{v}_1$, and $\bar{v}_2$ and make two observations. The first observation is that the A_x and A_x^0 terms disappear from Eq. (2.2.23) and (2.2.25) because $\gamma-1=\Gamma_x$ from A.7. The second is that Eq. (2.2.24) becomes $E_g=0$ because $g_x(V)=0$ from A.7 and $g_{Al}(V)=g_i(V)=0$ from A.8. In this case, Eq. (2.2.25) can be rewritten in a simpler form as

$$e=e_0-q_1\xi_1-q_2\xi_2+p\frac{v+B_1}{\gamma-1}+p\Delta B\frac{\xi_2}{\gamma-1} \tag{2.4.12}$$

by setting $e_x^0=e_0$, $q_3=q_1$, $q_{Al}^i=q_2$, $\lambda_3=\xi_1,\lambda_7=\xi_2$, $A_{Al}^0\bar{v}_1=B_1$, $A_i^0\bar{v}_2=B_2$ *and* $\Delta B=B_2-B_1$.

It is now convenient to derive the relationship between the adiabatic index k and γ. We consequently use the thermodynamic identiy for the sound speed and $c^2=kpv$, which yield

$$k\frac{p}{v}=\frac{p+\dfrac{\partial e}{\partial v}}{\dfrac{\partial e}{\partial p}}, \tag{2.4.13}$$

and equations for the partial derivatives of e derived from Eq. (2.4.12) to obtain the equation

$$k=\frac{\gamma v}{v+B_1+\Delta B\xi_2}. \tag{2.4.14}$$

We now use Eqs. (2.4.12), (2.4.14), and (the equations expressing the CJ conditions) Eqs. (2.4.5)-(2.4.8) to derive equations for steady state detonation parameters and, thereby, demonstrate the major problem we encounter in modeling nonideal detonations.

2.4.5. The Equations for Steady State (SS) Detonation Parameters

To derive equations for SS detonation parameters, we first combine Eqs. (2.4.14) and (2.4.5) to obtain an equation for the CJ volume v_j. Because Eq. (2.4.14) contains the reaction coordinate ξ_2, we are immediately faced with the main problem for this type of nonideal detonation, namely, that of determining how far the reaction of Al with the detonation products has progressed at the CJ point. To account for but not solve this problem, we assume that ξ_{2j} is a parameter to be determined and write our equation for v_j from Eq. (2.4.14) and (2.4.5) as

$$v_j=\frac{\gamma v_0-(B_1+\Delta B\xi_{2j})}{\gamma+1}. \tag{2.4.15}$$

The equation for $(k_j+1)^{-1}$ then follows by combining Eqs. (2.4.5) and (2.4.15) as

$$\frac{1}{k_j+1} = \frac{1+\frac{B_1}{v_0}+\frac{\Delta B}{v_0}\xi_{2,j}}{\gamma+1}, \tag{2.4.16}$$

and Eqs. (2.4.16) and (2.4.7) give the equation for the CJ pressure as

$$p_j = \frac{\rho_0 D^2[1+\frac{B_1}{v_0}+\frac{\Delta B}{v_0}\xi_{2,j}]}{\gamma+1}. \tag{2.4.17}$$

Equations (2.4.8), (2.4.12), (2.4.15), (2.4.16), and (2.4.17) then give the equation for the detonation velocity as follows. We first combine Eqs. (2.4.8) and (2.4.16) to obtain the equation

$$e_j - e_0 = \frac{D^2}{2(\gamma+1)^2}[1+\frac{B_1}{v_0}+\frac{\Delta B}{v_0}\xi_{2,j}]^2. \tag{2.4.18}$$

We then combine Eq. (2.4.12), with $\xi_1=1$ and $\xi_2=\xi_{2,j}$, and Eqs. (2.4.15) and (2.4.17) to obtain the equation

$$e_j - e_0 = -q_1 - q_2\xi_{2,j} + \frac{\gamma D^2}{(\gamma+1)^2}\frac{[1+\frac{B_1}{v_0}+\frac{\Delta B}{v_0}\xi_{2,j}]^2}{\gamma-1}. \tag{2.4.19}$$

The combination of Eqs. (2.4.18) and (2.4.19) then gives the equation for D as

$$D^2 = \frac{2(\gamma^2-1)(q_1+q_2\xi_{2,j})}{[1+\frac{B_1}{v_0}+\frac{\Delta B}{v_0}\xi_{2,j}]^2} \tag{2.4.20}$$

Eqs. (2.4.15)-(2.4.17) and Eq. (2.4.20) show explicitly that the value of $\xi_{2,j}$ must be known before SS detonation parameters can be calculated when all the other properties of the explosive composition are known. They also reduce to the equations for the two limiting cases of nonideal detonation discussed at the beginning of this section as follows. When the reaction of the Al with the explosive's products is very slow compared to the decomposition of the explosive, we can obtain the equations for the SS detonation parameters by setting $\xi_{2,j}=0$ in the above equations. When the reaction of the Al with explosive's products is appreciably faster than the decomposition of the explosive, we can obtain the equations for the SS detonation parameters by setting $\xi_{2,j}=1$ in the above equations.

In general, it is clear that an expression for the rate of reaction of the Al with the detonation products, $d\xi_2/dt$, must be known before the value of $\xi_{2,j}$ can be calculated and used in Eqs. (2.4.15)-(2.4.17) and (2.4.20) to calculate the SS detonation parameters for a nonideal detonation.

3. THE AP/Al/EXPLOSIVE GAS REACTIONS

3.1 The Al Reaction Model

The reaction of aluminum (Al) with air under normal ambient conditions is a well known phenomenon. Under these conditions a surface of pure Al will become coated with α-Al_2O_3 (corundum), which will grow in thickness to a few tens of Å in a few days. This process is electrolytic in nature has been extensively studied and is fairly well understood.[27-36]

In this process, a battery is formed with α-Al_2O_3 playing the role of solid electrolyte. The Al/Al_2O_3 interface is the battery anode, and the air $(O_2)/Al_2O_3$ interface, the cathode. At the anode, Al^{+3} ions (cations) are absorbed into Al_2O_3 and migrate toward the cathode. Likewise, at the cathode, $O^{=}$ ions (anions) may be absorbed and migrate toward the anode. Al_2O_3 is created through the interactions of the cations and anions.

One can view the current inside the Al_2O_3 in terms of the movement of cation vacancies (hereafter called vacancies) and vacancies in the electron band of the oxide[33] (hereafter called holes). Let μ_+ and μ_- be, respectively, the chemical potentials of the cation vacancies and electron holes, and let the Al_2O_3 be an infinite slab bounded by two parallel planes a distance l apart. Let x be the perpendicular distance from one plane and x=0, define the the anode surface (the Al/Al_2O_3 interface). The cathode surface (the Al_2O_3/O_2 interface) is then at x=l.

In the steady state of current flow, the number of cation vacancies passing through a plane perpendicular to x must be balanced by three times the number of holes passing in the opposite direction.

The system is functionaly a galvanic cell and obeys the same electrochemical laws. One therefore expects charge neutrality (or near neutrality) throughout the body of the electrolyte and, in addition, that the gradient of the chemical potential be balanced by the electrostatic force[33,37] that is,

$$\frac{d(\mu_+ + 3\mu_-)}{dx} = 3\epsilon e \ , \qquad (3.1.1)$$

where e is the electron charge and ϵ the electric field. The current density j in the cell is the sum of two terms, j_+ and j_-, which are equal. The current density j_+ is that for cation vacancies, and j_- for anion vacancies. The field ϵ is related to j via Ohm's law, i.e.,

$$j\rho = \epsilon \ . \qquad (3.1.2)$$

In Eq. (3.1.2), the resistivity ρ is the sum of two resistivities, ρ_+ and ρ_-, one for cations (or vacancies) and one for electrons (or holes). These have corresponding conductivities σ_+ and σ_-,so Eq. (3.1.2) can be written

$$j\left(\frac{1}{\sigma_+} + \frac{1}{\sigma_-}\right) = \epsilon = j\frac{\sigma_+ + \sigma_-}{\sigma_+\sigma_-} \ . \qquad (3.1.3)$$

Using this to substitute for ϵ in (3.1.1), one can solve for current density and find

$$j = \frac{\sigma_+\sigma_-}{3e(\sigma_+ + \sigma_-)} \frac{d(\mu_+ + 3\mu_-)}{dx} . \tag{3.1.4}$$

The growth of electrolyte (the creation of Al_2O_3) is simply related to j by

$$\frac{dl}{dt} = \frac{j\Omega_e}{6e} , \tag{3.1.5}$$

in which t is time, j/6e is half the number of cations plus corresponding holes passing through a unit area per unit time and Ω_e is the volume/molecule of Al_2O_3. Note that for σ_+ and σ_- one may use the basic semiconductor relationships

$$\sigma_+ = 3en_+\psi_+ \tag{3.1.6}$$

$$\sigma_- = en_-\psi_- , \tag{3.1.7}$$

in which $n_\pm$ and $\psi_\pm$ are, respectively, the number densities and mobilities for vacancies and holes. Because of the neutrality requirement, $n_+ = n_-$, and as will be shown further on, the derivative in Eq. (3.1.4) should equal $(4kT/n_+)dn_+/dx$, where k is the Boltzmann constant and T is temperature in °K. With these considerations, using (3.1.6) and (3.1.7) for σ_+ and σ_-, (3.1.4) becomes

$$j = \frac{4kT\psi_+\psi_-}{3\psi_+ + \psi_-} \frac{dn_+}{dx} . \tag{3.1.8}$$

One may properly assume $\psi_- >> \psi_+$ and integrate both sides of (3.1.8) between x=0 and x=l to obtain

$$j = 4kT\psi_+ \frac{n_+(l) - n_+(0)}{l} . \tag{3.1.9}$$

This expression for j contains calculable quantities on the right side and may be substituted into Eq. (3.1.5) to obtain the rate equation

$$\frac{dl}{dt} = \frac{K}{l} , \tag{3.1.10}$$

where the rate constant K is

$$K = 4\Omega_e kT\psi_+ \frac{n_+(l) - n_+(0)}{6e} . \tag{3.1.11}$$

Equation (3.1.10), when integrated, gives the parabolic rate law

$$l^2 = 2Kt . \tag{3.1.12}$$

One should note that in terms of the ionic conductivity σ_+, K has the form

$$K = 4\Omega_e kT \frac{\sigma_+(l) - \sigma_+(0)}{18e^2} . \tag{3.1.13}$$

These last four expressions are the basic model for the reaction rate of Al, which will be discussed and developed further in succeeding sections.

3.2 A Plausibility Argument Based on Existing Data

Experimentally, Al has been reacted with oxygen both in explosive detonations[38-43] and in controlled laboratory experiments.[32] Experiments[32] with flat slabs of pure Al in gaseous O_2 (at 76 torr) have been performed to temperatures above 800°K. The reaction product is on admixture of crystalline and amorphous γ-Al_2O_3, and the reaction rates even at the elevated temperatures are quite slow. The thickening of the products typically occurs at rates of a few microns per hour. The reaction rate constant grows with T, increasing by a factor of about 8 between 750°K and 850°K.

Growth rates follow a parabolic rate law until some limiting film thickness is reached. These thicknesses, typically 150Å to 200Å, increase linearly with temperature at very roughly 0.5Å per °K.

There are a number of relevant experiments involving aluminized explosives. These produce reaction results varying from partial to more or less complete reaction of Al. Some of this work involve AP and Al exclusively,[38,6,43] and in one effort a number of test samples are close to the theoretical maximum density (TMD).[43] In a few of the latter experiments, complete or nearly complete conversion of Al to Al_2O_3 is observed. Since the mean diameter of Al particles lies between 25μ and 30μ and the experimental time scale is of the order of 10μsec, the implied linear burning rate of Al is in the range of hundreds of cm per second. This is nine orders of magnitude greater than the μ/hour rate discussed above in the oxidation experiments and implies a rate constant 18 orders of magnitude greater than those observed. In the oxidation experiments, the reaction rate with temperature is seen to increase by a factor of about 8 over 100°K. At this rate of eight-fold increase, a factor of 10^{18} is achieved after a temperature increase of 2000°K. Since the maximum experimental oxidation rates for pure Al are observed at 850°K, the rates observed in explosive reactions should be reached at about 2850°K, which is in the proper range for explosive reaction products. In other words, a complex temperature extrapolation of the oxidation data moves it into the explosive regime, and this without regard to the O_2 pressure, which in an explosive is 10^6 times greater than the 76 torr in the oxidation experiments, further increasing the reaction rate. This, however, cannot be said of the limiting thicknesses of Al_2O_3 observed in these oxidation experiments. Linear extrapolation of these data to 2850°K indicates an increased thickness of about 450Å, which amounts to only a few hundredths of 1μ. Since explosive experiments do not observe such small limits, the thickness limits are either drastically affected by pressure or very nonlinear in temperature or both.

Another set of seemingly relevant[35] data involves the β-aluminas, which exhibit the phenomenon of anomalously high ionic conduction. In structure, these are basically slabs of crystalline γ-aluminum (about 10Å thick) separated by a layer or layers of monovalent metal oxide. Within this layer are "tunnels" through which ions can move rather freely. These materials exhibit conductivties as high as 0.1 $(\Omega cm)^{-1}$ at 1000°K. Using this value in (3.1.13), taking $\Omega_e \approx 4.3\times10^{-23}$, and assuming $\sigma_+(0)=0$, one can compute K and substitute into Eq. (3.1.12) to find l at 10 μsec. This yields $l \approx 70\mu$, a value also consistent with the results of explosive experiments.

All the above data can be utilized to piece together some plausible explanation of events in Al/explosive reactions. First of all, x-ray analysis of explosive products reveals[43] α-Al_2O_3 and

not the γ-Al_2O_3 observed in low pressure oxidation experiments (T<850°K). This makes some sense because γ-Al_2O_3 is known to transform to α-Al_2O_3 at elevated temperature, and moreover, α-Al_2O_3 is the denser of the two crystalline phases and should be preferred at very high pressures. The x-ray analyses, however, are qualitative and do not exclude amorphous Al_2O_3 in the explosive products, nor do they exclude some β-like form of γ-Al_2O_3, which may accrue due to the presence of monovalent metal impurities. The current model will assume, therefore, that both α-Al_2O_3 and some amorphous form of γ-Al_2O_3 are produced in the explosive gases. The general Al_2O_3 products will be considered to contain tunnel structures through which Al^{+3} cations can readily pass and from which $O^{=}$ are excluded because of their much larger ionic radius (2.5 times that of Al^{+3}). The very last assumption is made with the knowledge that if significant reaction occured at the Al/oxide interface it would have little effect on the explosive gases because of the time necessary for the heat of reaction to conduct outward through the Al_2O_3 product layer. This time is about βl^2 where β is reciprocal diffusivity. For Al_2O_3, $\beta \approx 900$ sec/cm^2, so that the time for the reaction heat to pass through 1μ of product film is 9 μsec or about the full length of an explosive experiment. Eventually, the energy escapes, but there would be little effect on the overall release isentrope of the explosive gases and, therefore, on preformance.

The only term in Eq. (3.1.11) that can account for the huge increase in K under explosive conditions is the cationic mobility ψ_+. In γ-Al_2O_3 (and presumably in α-Al_2O_3), this has an Arrhenius-like temperature dependence, which cannot explain the increase in question unless the activation energy itself decreases drastically. Since the activation energy is a measure of the energy barrier a cation must overcome to change sites, one would expect an increase in this barrier energy with pressure (decreasing volume) as opposed to a decrease. If barrier height, however, did decrease in some unusual way with decreasing volume, the relative incompressibility of α-Al_2O_3 , which is gem-like, would prevent much change from occuring. The postulation of tunnels as cation conduits seems necessary to obtain lower activation energies for cation motion because of the relative incompressibility of α-Al_2O_3, and because the temperature extrapolation discussed above is highly nonlinear (and not very credible) and leads us to the very highest part of the range of detonation temperatures. Al is known to react agressively with oxygen at much lower temperatures (but above about 1000°K).

In summary, interpretation of the data discussed above leads to the following preliminary reaction model:

1. Tunnel structures, which conduct Al^{+3} cations, are assumed to form naturally with the Al_2O_3 reaction products in detonated Al/explosive compositions.

2. Anions are excluded from the conducting tunnels

3. The solid reaction products are assumed to be an admixture of α-Al_2O_3, amorphous Al_2O_3, and, possibly, some β form.

3.3 Equilibrium at the Cathode and Anode

At the anode, Al atoms enter Al_2O_3 as Al^{+3} ions giving 3 electrons to the Al_2O_3 bands, i.e., within the Al_2O_3,

$$Al \rightleftarrows Al^{+3} + 3e \ . \tag{3.3.1}$$

At the cathode, Al^{+3} reacts with O_2 to form Al_2O_3, i.e.,

$$6e + 2Al^{+3} + \frac{3}{2}O_2 \rightleftarrows Al_2O_3 + 2V_+ + 6V_- \ , \tag{3.3.2}$$

where V_+ represents a cation vacancy and V_- a hole in the electron bands. The equilibrium in these reactions may be used to find the quantity n_+ in Eq. (3.1.11). To simplify the process, subscripts will be assigned to connect the properties of a constituent with the constituent. The subscript e will detonate properties of Al_2O_3 (such as Ω_e). In addition, a, x, c, and q will designate properties of Al, O_2, Al^{+3} and electrons, respectively. As before, + and - will describe properties of vacancies and holes.

At equilibrium, for the reaction Eq. (3.3.1), one can write[37,44]

$$\mu_a = \mu_c + 3\mu_q \ , \tag{3.3.3}$$

where the μ are the indicated chemical potentials. Likewise for reaction Eq. (3.3.2), one has

$$6\mu_q + 2\mu_c + \frac{3}{2}\mu_x = \mu_e + 2\mu_+ + 6\mu_- \ . \tag{3.3.4}$$

From statistical mechanics,[37,44] one knows that for a unit of the constituent k,

$$\mu_k = -kTln\frac{q_k}{N_k} \ , \tag{3.3.5}$$

where q_k is the partition function per unit, N_k is the number of the units that are indistinguishable from one another, and N_k=1 if they are all distinguishable.

In this regard, both the atoms of Al in the metal and the molecules of Al_2O_3 in the electrolyte are completely distinguishable because of their fixed positions. This also applies to the electrons in the electrolyte energy bands, which are distinguishable by their quantum numbers. Therefore,

$$N_a = N_c = N_q = 1 \tag{3.3.6}$$

On the other hand, vacancies, holes, and O_2 molecules are completely indistiguishable because they have neither fixed positions nor quantum numbers. Therefore, N_x, N_+ and N_- are simply equal to the respective numbers of these constituents.

The situation for cations travelling in tunnels is more complex because cations within a given tunnel are indistinguishable, but cations in different tunnels can be distinguished. This subject is treated next.

3.4 The Partition Function Per Cation

In travelling from anode to cathode a cation will be assumed to traverse a tunnel of (mean) length l_t. Since the system is expected to be at high temperature, it is described by the semiclassical grand partition function[44]

$$Q_c = \frac{1}{h^{3w}(w_t!)^{N_t}} \int \cdots \int e^{-\beta H(p,q)} dp_1 dq_1 \cdots dp_w dq_w \ . \qquad (3.4.1)$$

Here h is Planck's constant, p,q are the momentum and space coordinates, respectively, $\beta=1/kT$, w is the total number of cations, w_t is the number of cations per tunnel, N_t is the number of tunnels, and H is the Hamiltonion. How Eq. (3.4.1) is evaluated depends on the configuration of the tunnels. If they are very wide and high compared to the Al^{+3} diameter ($\approx$1Å), then the cation can be viewed as bouncing from the tunnel walls while traversing the length. If the width and/or height are relatively narrow, then the cation may be vibrating transversely in one or both directions while travelling the length. Along the tunnel length, there may be barriers to motion that must be overcome. Let the distance between barriers be *s* and the distance across a barrier be s_b. Also, let the barrier height be ϵ_b. Assume, as well, that the tunnel is narrow in either or both of the two transverse directions and that the ion oscillates harmonically in these directions with frequencies ν_h and ν_w for the height and width, respectively. The number of cations w_t within a tunnel is expected to be small relative to the number of sites of length $s+s_b$. This being the case, the Hamiltonion H_c of a single cation can be written as

$$H_c = \frac{p^2}{2m_c} + 4\pi^2\nu_q^2\frac{q^2}{2} + \epsilon_c^0 + g(q)\epsilon_b \ , \qquad (3.4.2)$$

where m_c is the cation mass, ϵ_c^0 is the potential of the cation within the tunnel when in the region of length s between barriers, the function g(q) is zero within the region s and equals one in the barrier region s_b, and the oscillation frequecy ν_q is assumed to be zero if q is in a direction of large tunnel width or height.

Using Eq. (3.4.2) in Eq. (3.4.1) for a *single* cation, the integration can be performed over the three space and three momentum coordinates, yielding the integral

$$I_c=(2\pi m_c kT)^{\frac{3-V_h-V_w}{2}} \left(\frac{kT}{\nu_h}\right)^{V_h} \left(\frac{kT}{\nu_w}\right)^{V_w} x_h^{1-V_h} x_w^{1-V_w} e^{-\beta\epsilon_c^0} \frac{s_1+s_b e^{-\beta\epsilon_b}}{s_1+s_b} l_t \ . \qquad (3.4.3)$$

In this expression, the indices V_h, V_w are unity if the height h or width w of the tunnel are small enough to cause transverse harmonic vibrations of the cation, and are zero otherwise. One should also note that the ratio $l_t/(s_1+s_b)$ is just the number of sites of length $s+s_b$ within a tunnel. This ratio carries the integration over a single site through the entire tunnel length.

The integral Eq. (3.4.3) is over the coordinates of a single cation. If integration is performed for *all cations within a tunnel* one obtains $(I_c)^{w_t}$. Doing this for *all tunnels*, one obtains $(I_c)^{N_t w_t}$ for the multiple integral in Eq. (3.4.1). Since

$$w = N_t w_t \ , \qquad (3.4.4)$$

then Eq. (3.3.7) can be rewritten as

$$Q_c = \frac{I_c^w}{(w_t!)^{N_t} h^{3w}} \ . \qquad (3.4.5)$$

Using the Stirling approximation

$$w_t! \approx w_t^{w_t} e^{-w_t} \sqrt{2\pi w_t} \tag{3.4.6}$$

and remembering that $N_t w_t = w$, one finds

$$(w_t!)^{N_t} \approx w_t^{w} e^{-w} (2\pi w_t)^{\frac{N_t}{2}} \tag{3.4.7}$$

The Hemholtz energy for the cations A_c is given by

$$A_c = -kT \ln Q_c \ . \tag{3.4.8}$$

Substituting Eq. (3.4.7) into Eq. (3.4.5) for Q_c, one finds for A_c,

$$A_c = -kTw[\ln \frac{I_c}{h^3 w_t} + 1 - \frac{N_t}{2w} \ln(2\pi w_t)] \ . \tag{3.4.9}$$

Since $N_t/w << 1$, one can neglect the last two terms in the brackets, and A_c becomes

$$A_c = -kTw \ln \frac{I_c N_t}{h^3 w} \ . \tag{3.4.10}$$

Using Eq. (3.4.10), one can obtain the chemical potential for cations from the relation

$$\mu_c = \frac{\partial A_c}{\partial w} \ , \tag{3.4.11}$$

which on neglecting small terms yields

$$\mu_c = -kT \ln \frac{I_c N_t}{h^3 w} \ . \tag{3.4.12}$$

Relating Eq. (3.4.12) to Eq. (3.3.5), one can see that

$$q_c = \frac{I_c}{h^3} \tag{3.4.13}$$

and

$$N_c = \frac{w}{N_t} = w_t \ . \tag{3.4.14}$$

This completes the statistical description of cations; the development is necessary because it is specific to the model and has not previously been done. The partition functions of the remaining constituents are better understood and are given below.

3.5. The Evaluation of the Remaining Partition Functions: q_a, q_e, q_q, q_+, q_-, q_x

Subsequent to shocking, the unreacted Al is expected to be above its Debye temperature. So for q_a, we find

$$q_a = (\frac{T}{\theta_c})^3 e^{-\beta \epsilon_w^0} \ , \tag{3.5.1}$$

where θ_c is the Debye temperature divided by the cube root of the base of the natural logrithm

and ϵ_a^0 is the potential energy/atom of Al in the metal at 0°K (a function of volume only) plus the energy required to transfer three electrons to the Al_2O_3 band. For Al_2O_3, a single Debye temperature will be assigned to the vibrational modes per degree of freedom of the molecule (3 associated with translation and 3 with rotation). For these acoustic modes, T is again expected to be greater than the assigned Debye temperature. For each of the nine remaining vibronic modes, an Einstein temperature θ_e is assigned. This gives for q_e,

$$q_e = (\frac{T}{\theta_e})^6 [\prod_{i=1}^{9} \frac{e^{-\frac{\theta_i}{2T}}}{1-e^{-\frac{\theta_i}{T}}}] \; e^{-\beta[\epsilon_e^b+\epsilon_e^0]} \; , \tag{3.5.2}$$

where θ_e is defined in the same manner as for Al, the θ_i are the nine Einstein temperatures, ϵ_e^b is the binding energy of the Al_2O_3 molecule, and ϵ_e^0 is the potential of the molecule in the Al_2O_3 lattice.

The electron partition function q_q is quite simply

$$q_q = e^{-\beta\epsilon_q^0} \tag{3.5.3}$$

in which ϵ_q^0 is the energy binding the electron in the Al_2O_3 band. The functions q_+ and q_- are[45]

$$q_+ = N_e e^{-\beta\epsilon_+^0} \tag{3.5.4}$$

and

$$q_- = N_e e^{-\beta\epsilon_-^0} \; . \tag{3.5.5}$$

The quantities ϵ_+^0 and ϵ_-^0 are the negatives of ϵ_c^0 and ϵ_q^0, respectively.

The partition function q_x for O_2 gas is

$$q_x = (\frac{2\pi m_x kT}{h^2})^{\frac{3}{2}} \; V_x e^{-\beta[\epsilon_x^b+\epsilon_x^0]} \; , \tag{3.5.6}$$

where m_x is the mass of an O_2 molecule, V_x the gas volume, ϵ_x^b the binding energy of O_2, and ϵ_x^0 the nonthermal potential energy of the O_2 molecule in the gas.

3.6. The Evaluation of n_+

Using Eq. (3.3.3), which describes equilibrium at the anode, along with Eq. (3.3.5) for the chemical potentials, Eq. (3.3.3) becomes

$$\ln\frac{q_a}{N_a} = \ln\frac{q_c}{N_c} + \ln(\frac{q_q}{N_q})^3 = \ln\frac{q_c q_q^3}{N_c N_q^3} \; , \tag{3.6.1}$$

or since (from Eq. (3.3.6) and Eq. (3.4.14)) $N_a=N_q=1$ and $N_c=w_t$,

$$q_a = \frac{q_c q_q^3}{w_t} . \tag{3.6.2}$$

In an entirely similar manner for Eq. (3.3.4), one has

$$\ln \frac{q_q^6 q_c^2 q_x^{3/2}}{w_t^2 N_x^{3/2}} = \ln \frac{q_e q_+^2 q_-^6}{N_+^2 N_-^6} . \tag{3.6.3}$$

Setting the logrithmic arguments equal in Eq. (3.6.3) and solving for $N_+^2 N_-^6$ gives

$$N_+^2 N_-^6 = \frac{q_e q_+^2 q_-^6 N_x^{3/2} w_t^2}{q_q^6 q_c^2 q_x^{3/2}} . \tag{3.6.4}$$

The quantity q_c/w_t may be solved for in Eq. (3.6.2) and substituted into Eq. (3.6.4), and since charge neutrality is specified, one can set $N_-=3N_+$, with the result

$$3^6 (N^+)^8 = \frac{q_e q_+^2 q_-^6 N_x^{3/2}}{q_a^2 q_x^{3/2}} . \tag{3.6.5}$$

The partition functions given in Section 3.5 may now be substituted into Eq. (3.6.5), after which one finds

$$(N_+)^8 = \frac{N_e^8 (\frac{N_x}{V_x})^{\frac{3}{2}} (\frac{T_e \theta_a}{3 T_a \theta_e})^6 q_{ev} \exp[-\beta(\epsilon_e^b + \epsilon_e^0 + 2\epsilon_+^0 + 6\epsilon_-^0 - 2\epsilon_a^0 - 1.5\epsilon_x^0 - 1.5\epsilon_x^b)]}{(\frac{2\pi m_x kT_x}{h^2})^{9/4}} . \tag{3.6.5}$$

In this, the temperatures T apply to the components indicated by the subscripts, and q_{ev} is defined as

$$q_{ev} = \prod_{i=1}^{9} \frac{e^{-\frac{\theta_i}{2T}}}{1 - e^{-\frac{\theta_i}{T}}} . \tag{3.6.6}$$

Equation (3.6.5) may be divided by V_e^8 to convert the total numbers N into number densities n. Moreover, because of the gem-like quality of Al_2O_3, the quantities that depend only on the volume of the electrolyte can be viewed as constant even at detonation pressures. These quantities include the ϵ's associated with Al_2O_3 and its enclosed ions, electrons, and vacancies. They may be factored in Eq. (3.6.5) into a constant along with other constants such as the binding energy of O_2, m_x, h, etc. Thus, the solution of Eq. (3.6.5) for n_+ is

$$n_+ = \Gamma n_e e^{-\beta\rho} n_x^{3/16} (\frac{\theta_a T_e}{\theta_e T_a})^{3/4} \exp[-\frac{\beta}{8}(-2\epsilon_a^0 - 1.5\epsilon_x^0)] \frac{q_{ev}^{1/8}}{T_x^{9/32}} . \tag{3.6.7}$$

Here, $\rho = \epsilon_e^b + \epsilon_c^0 + 2\epsilon_+^0 + 6\epsilon_-^0 - 1.5\epsilon_x^b$ and

$$\Gamma = 3^{-3/4}\left(\frac{2\pi m_x k}{h^2}\right)^{-9/32} \tag{3.6.8}$$

are constants. The quantity n_+ in Eq. (3.6.7) is the same as $n_+(l)$ in Eq. (3.1.11) and can be reasonably evaluated except for the constant ρ, which can be experimentally determined. Attention is turned next to the cationic mobility ψ^+.

3.7. The Evaluation of ψ^+.

The cationic mobility is related to the velocity of cations parallel to the walls of the tunnels described in Section 3.4. The concepts and notation in that development are used here to find ψ^+.

Consider a cation situated within a tunnel site. The probability that it has a kinetic energy parallel to the tunnel walls with some velocity component toward the cathode, which is greater than the barrier height ϵ_b, is

$$p_r = \frac{\int_{\sqrt{2m_c\epsilon_b}}^{\infty} e^{-\beta\frac{p^2}{2m_c}}dp}{\int_{-\infty}^{\infty} e^{-\beta\frac{p^2}{2m_c}}dp} . \tag{3.7.1}$$

The average value of the velocity, $\bar{v}$, in the same direction for energies greater than ϵ_b is

$$\bar{v} = \frac{kT\int_{\sqrt{2m_c\epsilon_b}}^{\infty} \frac{p}{m_c kT} e^{-\beta\frac{p^2}{2m_c}}dp}{\int_{\sqrt{2m_c\epsilon_b}}^{\infty} e^{-\beta\frac{p^2}{2m_c}}dp} . \tag{3.7.2}$$

Tunnels are assumed to extend from anode to cathode, but are not necessarily parallel to the x-axis of the electrolyte. If the tunnel consists of segments forming various angles at their joints, the velocity in Eq. (3.7.2) must be ultimately corrected to give the value in the direction of the current (parallel to the x axis). For example, if lines parallel to all tunnel segments at some value of x form random angles with the x-axis, varying between $\pi/2$ and $-\pi/2$, then $4\bar{v}/\pi^2$ will give the average velocity with which cations pass from one site to another in the positive x-direction. For the moment, assume this is the case. Then the number of cations/sec per cm^2, i_+, passing through a plane perpendicular to the x-axis toward the cathode at position x is

$$i_+ = \frac{4}{\pi^2} n_c(x) p_r \bar{v} . \tag{3.7.3a}$$

In the product $p_r\bar{v}$, the nonintegrable numerator in Eq. (3.7.1) and denominator in Eq. (3.7.2) cancel. The remaining integrals are easily evaluated, giving

$$p_r\bar{v} = (\frac{kT}{2\pi m_c})^{1/2} e^{-\frac{\epsilon_b}{kT}} . \qquad (3.7.3b)$$

If an electric field ϵ points in the positive x-direction, the barrier heights are lowered toward positive x due to the electric potential. The barrier to the right (greater x) of the point x in any tunnel is lowered by $3\epsilon e(s+s_b)$ relative to the barrier to the left. In this case, using Eqs. (3.7.3a) and (3.7.3b) the ionic current j_r moving toward positive x is

$$j_r = 3en_c \frac{4}{\pi^2}(\frac{kT}{2\pi m_c})^{1/2} e^{\frac{-\epsilon_b + 3e\epsilon(s+s_b)}{kT}} . \qquad (3.7.4)$$

The current toward negative x, j_l, is identical, except there is no electric term in the exponential. The net ionic current $j_+ = j_r + j_l$ is, therefore,

$$j_+ = 3en_c \frac{4}{\pi^2}(\frac{kT}{2\pi m_c})^{1/2} e^{-\frac{\epsilon_b}{kT}} [e^{\frac{3e\epsilon(s+s_b)}{kT}} - 1] . \qquad (3.7.5)$$

One expects the electric potential to be small relative to kT, allowing a two-term expansion of the exponential. This gives

$$j_+ = 3en_c \frac{4}{\pi^2}(\frac{kT}{2\pi m_c})^{1/2} e^{-\frac{\epsilon_b}{kT}} \frac{3e\epsilon(s+s_b)}{kT} . \qquad (3.7.6)$$

Because of the definition of the mobility ψ^+ (the cation velocity/unit electric field), one also has

$$j_+ = 3en_c\psi^+\epsilon . \qquad (3.7.7)$$

Setting Eq. (3.7.6) and Eq. (3.7.7) equal and solving for ψ^+, the result is

$$\psi^+ = \frac{12e}{\pi^2}(s+s_b)(2\pi m_c kT)^{-1/2} e^{-\epsilon_b/kT} . \qquad (3.7.8)$$

This result, proportional to $T^{-½}$, is somewhat different for the usual form[35] that is proportional to T^{-1}. The change stems directly from the fact that the cations are allowed to move freely between tunnel barriers, whereas in the usual derivation, they oscillate harmonically in a site before jumping to the next.

One should note that the assumed tunnel structure (random joint angles, etc.) may not be accurate, but differences in configurations are expected to change ψ^+ only by a multiplicative constant.

With Eq. (3.7.8) for ψ^+ and Eq. (3.6.7) for n_+, Eq. (3.1.11) for K is evaluated except for the quantity $n_+(0)$, which is assumed here to be negligably small. This is because for $n_+(0)$ to be significant, it would require Al to be separated from Al_2O_3 at the anode with no oxygen present. This is a highly improbable reaction, so $n_+(0)$ will be neglected. In writing a final expression for K, the quantity n_e has to be set equal to $1/\Omega_e$, constant terms are again grouped for convenience, and the electrolyte temperature T_e is assigned to the expression for ψ^+. The result for K is

$$K = \Gamma_1 e^{-\frac{\rho_1}{kT_f}} n_x^{3/16} \theta_a^{3/4} \left(\frac{T_e^{5/4}}{T_a^{3/4} T_x^{9/32}}\right) q_{ev}^{1/8} e^{\frac{2\epsilon_a^0 + 1.5\epsilon_x^0}{8kT_f}}, \qquad (3.7.9)$$

where

$$\Gamma_1 = \theta_e^{-3/4} \frac{8}{\pi} k(s+s_b)(2\pi m_c)^{1/2}\Gamma \qquad (3.7.10)$$

and

$$\rho_1 = \rho + \epsilon_b \ . \qquad (3.7.11)$$

The O_2 number density n_x is proportional to total pressure p. Note that the 3/16 power is close to the 1/6 power heuristically attached to explosive experiments by Guirguis and Miller.[38] The temperature structure of Eq. (3.7.9) is unusual. If all elements were at the same temperature (T_f=Te=Ta=Tx), the exponential coefficient would vary as $T_f^{7/32}$, where T_f is the product gas (fluid) temperature in Section 2. This will be the case in the detonation model of Section 2. Because Al_2O_3 forms at the Al_2O_3/fluid interface and there dissipates its excess energy, it is reasonable to assume the bulk Al_2O_3 and fluid temperatures are roughly equal. Moreover, at the Al/Al_2O_3 interface, one expects at least some small depth of Al to be at the same temperature as Al_2O_3. Thus, in this model, T_e=T_a=T_x=T_f.

Clearly, the derivation of Eq. (3.7.9) neglects the intermediate oxidation states of Al, which must occur before the formation of Al_2O_3. These have been assumed to be sufficiently short-lived so as to have little effect on the rate constant. This subject will be examined further in a future Phase II effort.

Before leaving this subject, it should be mentioned that, for convenience, the ϵ's in the exponents of Eq. (3.7.9) have been expressed in terms different from the heats of formation in Section 2. Nevertheless, the two are directly related, and the transformations are easily made if one wishes to do so. For example, the heat of formation of Al_2O_3, $(\Delta H_{f_0}^0)_{Al_2O_3}$, at 0°K and 1 atmosphere is per mole,

$$(\Delta H_{f_0}^0)_{Al_2O_3} = -A\left\{\left[\epsilon_a^0 + \frac{3}{2}(\epsilon_x^0 + \epsilon_x^b)\right] - (\epsilon_e^0 + \epsilon_e^b)\right\},$$

where A is Avogadro's number, and the small pV terms have been neglected.

3.8 The Al Reaction Fraction λ As a Function of Time.

The equations developed thus far for the reaction of Al have been restricted to Al slabs. In this calculation, identical spheres of Al are assumed in a mixture of Al and AP. Immediately behind the detonation front, these spheres will have radius r_h, smaller than their initial radius r_0. In the bath of hot product gas, Al_2O_3 will grow on the sphere. Let the composite sphere have radius R; the enclosed Al have radius r_a; r be any specific radius in the composite; the current density in the electrolyte be j(r).

j(r) will be dominated by the Al surface area and decrease with increasing r such that the

total current is constant. That is,

$$j(r) = \frac{r^2}{R^2} j(R) \ . \tag{3.8.1}$$

Using Eq. (3.1.8) for j(r) (with $\psi_- >> \psi_+$), one has

$$\frac{r^2}{R^2} j(R) = 4kT\psi_+ \frac{dn_+}{dr} \ . \tag{3.8.2}$$

Integration of Eq. (3.8.2) between r_a and R yields, after some rearrangement (and neglecting $n_+(r_a)$),

$$j(R) = 12kT\psi_+ \frac{n_+(R)}{R} (1-\frac{r_a^3}{R^3})^{-1} \tag{3.8.3}$$

The time derivative of the Al radius is (Ω_a=volume/atom of Al),

$$\frac{dr_a}{dt} = -j(r_a)\frac{\Omega_a}{3e} = -\frac{r_a^2}{R^2} j(R) \ \frac{\Omega_a}{3e} \ . \tag{3.8.4}$$

Or, using Eq. (3.8.3) for j(R),

$$\frac{dr_a}{dt} = -\frac{r_a^2}{R^2} \ \frac{\Omega_a}{3e} \frac{12kT\psi_+ n_+(R)}{R} \ (1-\frac{r_a^3}{R^3})^{-1} \ . \tag{3.8.5}$$

Using the formula for K in Eq. (3.1.11) (with $n_+(0)=0$), one can write Eq. (3.8.5) in the form

$$\frac{dr_a}{dt} = -\frac{3(\frac{2\Omega_a}{\Omega_e})K}{R(1-\frac{r_a^3}{R^3})} \ . \tag{3.8.6}$$

From Section 2, the reacted fraction of Al is $\lambda=1-r_a^3/r_h^3$. Therefore,

$$\frac{d\lambda}{dt} = -3\frac{r_a^2}{r_h^3} \ \frac{dr_a}{dt} \ . \tag{3.8.7}$$

Substitution of Eq. (3.8.6) into Eq. (3.8.7) gives

$$\frac{d\lambda}{dt} = 18(\frac{\Omega_a}{\Omega_e})K\frac{r_a^2/r_h^2}{r_h R} \ (1-\frac{r_a^3}{R^3})^{-1} \ . \tag{3.8.8}$$

Now note that the volume increase of Al_2O_3 is $\Omega_e/2\Omega_a$ times the volume change of Al. This leads to

$$R^3 - r_a^3 = \frac{\Omega_e}{2\Omega_a} \ (r_h^3 - r_a^3) \ . \tag{3.8.9}$$

From Eq. (3.8.9) and the definition of λ, one can show that

$$R(1-\frac{r_a^3}{R^3}) = \frac{\Omega_e}{2\Omega_a}\lambda\frac{r_h^3}{R^2} \tag{3.8.10}$$

and

$$R = r_h[1-\lambda+\frac{\Omega_e}{2\Omega_a}\lambda]^{1/3} . \tag{3.8.11}$$

Using Eq. (3.8.9) for the described quantity in (3.8.8) and replacing the resulting R with Eq. (3.8.11), one finally obtains Eq. (3.8.7) in the form (note $r_a^2/r_h^2 = (1-\lambda)^{2/3}$)

$$\frac{d\lambda}{dt} = \frac{9(\frac{2\Omega_a}{\Omega_e})^2K(1-\lambda)^{2/3}[1-\lambda+\frac{\Omega_e}{2\Omega_a}\lambda]^{2/3}}{r_h^2\lambda} , \tag{3.8.12}$$

With K given by Eq. (3.7.9) and $2\Omega_a/\Omega_e$ by $2V_1/V_2$ (from Section 2), *this completes the rate equation for the Al reaction.* The reaction is assumed to occur only with the O_2 in the explosive gases. Reactions between Al and other species are expected but are considered much less probable because they are energetically less favorable. Except for the variation with gas pressure, Eq. (3.8.12) does not resemble the heuristic fit for $d\lambda/dt$ mentioned earlier.[38] In the latter, $d\lambda/dt$ is found proportional to $(1-\lambda)^{1/2}$, which it clearly is not in Eq. (3.8.12). K, however, has a significant temperature and volume dependence, so in the end, Eq. (3.8.12) may show the observed behavior.

The sensitivity of the reaction rate with temperature may explain the reaction delays directly and indirectly observed in many explosive experiments. Immediately behind the shock front of a detonation, the temperature may not be high enough to cause rapid reaction. Nevertheless, as reaction proceeds, temperatures may increase to the point of rapid acceleration of reaction. This type of process would generally seem like a reaction delay.

3.9. The Reaction Rate of AP

Consider a system composed of uniform AP spheres of radius a. At the front of a plane detonation wave passing through the system, the spheres will be deformed into polyhedra with no intervening pore spaces. Let these be approximated by spheres of radius a_H. The polyhedra surfaces, due to friction generated at the interfaces and due to pore collapse, should be at a very high temperature T_s. This is assumed to cause immediate reaction at the surface with the production of products at temperature T_f. The unreacted molecules, at temperature T_{AP} adjacent to the products, will receive thermal energy from them, but it will take a certain critical time τ_c for sufficient energy to reach the intramolecular vibrational modes of the AP molecules to cause reaction and produce equilibrium products. This time delay τ_c will precede the transmission of reaction from one molecular surface layer to the next. If the molecular separation is Δ, then the reaction proceeds at the rate $d\rho/dt=-\Delta/\tau_c$, where ρ is the radius of the sphericalized polyhedra of unburned AP and t is time. The fraction of AP reacted at any time is $\lambda_1=1-\rho^3/a_H^3$. One can combine these last two equations to find, $d\lambda_1/dt$, and obtain

$$\frac{d\lambda_1}{dt} = \frac{3(1-\lambda_1)^{2/3}}{(a_H/\Delta)\tau_c} \quad . \tag{3.9.1}$$

The critical time delay of τ_c devolves from three basic processes. The first is a process of heat conduction (thermal diffusion) by which energy is transferred from the product gas at T_f to the unreacted AP at T_{AP}, raising the temperature of the latter. The second is a thermal relaxation process in which energy is transferred from the acoustic vibrational modes into the vibronic (intramolecular) modes of unreacted AP. The third is a process by which the AP is reduced to products once reaction has begun. Each of these processes takes time and contributes to τ_c. The time τ_D for the first process is approximately $\beta\Delta^2$, where β is the reciprocal of the diffusivity of AP. At standard temperature and pressure (STP), $\beta \approx 601$ sec/cm^2 and $\Delta \approx 5.8A^0$, which makes τ_D of the order of 2 ps. This time is too small to govern the reaction rate of AP, which in 9μ-sized particles is known[6] to react in about 0.5 μsec under detonation conditions. If τ_c were equal to τ_D, this reaction would occur in 15 ns. One should therefore expect that the unreacted AP adjacent to product gas reaches highly elevated temperature well before reaction proceeds to products.

The second process is governed by a relation of the type[46]

$$T_c - T_{AP} = \xi^{-2}\theta^2 T_f \left(\frac{T_f}{\theta^2}\right)^{\delta-1} \frac{\tau_R^2}{\delta!} \quad , \tag{3.9.2}$$

where T_c is some critical temperature associated with the energy an AP molecule must reach before reaction begins promptly (in say less that 1 ps). θ is the Debye temperature of the acoustic modes in AP, δ is the ratio of the Einstein temperature of the lowest frequency vibronic mode, θ_E, to θ(i.e., $\delta=\theta_E/\theta$), and ξ is a constant characteristic of AP.

When both sides of Eq. (3.9.2) are multiplied by k, and τ_R is replaced by t, it represents the energy poured into the lowest frequency vibronic mode in time t by a neighboring molecule at temperature T_f. The process stops when the energies are in balance. One expects this relatively slow process to determine the rate at which energy transfers into vibronic modes.

For $\delta!$ in Eq. (3.9.2), one may use the Stirling formula, which is reasonably accurate even for $\delta=1$. So set

$$\delta! = \delta^{\delta} e^{-\delta} (2\pi\delta)^{1/2} \quad . \tag{3.9.3}$$

The temperature θ_E in delta may be determined from spectral data on AP, and θ, which varies with volume, can be expressed in terms of the Gruneisen parameter γ_a for the highest frequency AP acoustic modes. By definition,

$$\gamma_a = \frac{-d(\ln\theta)}{d(\ln v_{AP})} \quad . \tag{3.9.4}$$

When integrated, this gives

$$\theta = \theta_0 \exp\left[-\int_{v_0}^{v_{AP}} \frac{\gamma_a}{v'_{AP}}\, dv'_{AP}\right] \quad . \tag{3.9.5}$$

Reasonable expressions[47,48] for γ_a may be derived from the equation of state of AP.[11] Thus, δ and θ can be determined as a function of v_{AP}.

Solving for τ_R in Eq. (3.9.2), using Eq. (3.9.3) for δ!, one has

$$\tau_R = \frac{\xi T_f^{1/2}}{\theta^2} [\delta^{\delta} e^{-\delta} (2\pi\delta)^{1/2} (\frac{\theta^2}{T_f})^{\delta} \frac{T_c - T_{AP}}{T_f}]^{1/2} . \qquad (3.9.6)$$

This represents the time required for a molecule of AP at $T=T_{AP}$ to react when adjacent to molecules at $T=T_f$. The quantities ξ and T_c are constants related to AP only and must be experimentally determined. It should be noted that the relation Eq. (3.9.2) is classically developed.[46] Except for a multiplicative constant (near 1), the quantum mechanical analogue is identical.

The third process contributing to τ_c involves the time τ_e necessary for reaction to proceed to equilibrium products at T_f, when the average molecular temperature is sufficient to initiate reaction at the beginning of the process. This time should be some multiple of the time it takes a molecular fragment to collide with another molecule. In AP at STP, the separation between molecules is about 5.8Å, but the molecules themselves have dimensions (sphericalized diameters) of about 3.36 Å. So the average distance to collision for a fragment is about 2.5Å at a velocity of roughly $(kT_f/m_f)^{½}$, where m_f is the fragment mass.

Taking T_f to be (a conservative) 1000°K, the time between collisions for, say, an NH_4 fragment is about 0.4 ps. If ten collisions are required to convert the fragment components into parts of equilibrium products, then only 4 ps is the requisite time. In view of this, it seems reasonable to assume that the first and third processes contributing to τ_c are small compared to the second, which is in the approximate range 10-120 ps[25,49] and that τ_c can be represented by

$$\tau_c = \tau_R + \tau' , \qquad (3.9.7)$$

where $\tau' = \tau_D + \tau_e$ and is treated as a constant with a value between about 2 ps and 10 ps.

4. CONCLUSIONS AND SUMMARY

4.1. Technical Results

Theoretical work was performed to formulate a first generation model for nonideal detonation that is based on fundamental physical principles and can be used to investigate the nonideal detonation process in explosive compositions containing Al.

In the portion of this work presented in Section 2, we formulated the thermo-hydrodynamics that is needed to treat reacting AP/Al and CHNO/Al compositions and account for the decomposition of these explosives and the subsequent reactions of their products with Al. We also considered the relationship between the steady-state reaction zone length and reaction time in AP, and developed a prototype model for steady-state, nonideal detonation in a CHNO/Al composition.

In our Phase I approach to reactions in these AP/Al and CHNO/Al compositions, single-reaction coordinates were used to describe the decompositions of the AP and the CHNO explosive, and a single reaction coordinate was used to describe the reactions of their products with Al to form either α-Al_2O_3 (corundum) or amporphous γ-Al_2O_3. The second reaction coordinate for the AP/Al composition was assigned to the reaction of Al with O_2; the second reaction coordinate for the CHNO/Al composition was assigned to the reaction of Al with H_2O and C, with the H_2 produced from the H_2O reacting with the C to form C_2H_6. Although these reaction schemes are clearly limited, they are more realistic than some empirical treatments of Al reactions in hydrocodes, because they account explicitly for the conservation of mass as the Al removes oxygen from the detonation products.

The mass-balance equations for these reaction schemes were used to construct constitutive equations for the specific internal energies of our reacting AP/Al and CHNO/Al mixtures, with each of their components governed by its own equation of state (EOS). Generalized Mie-Gruneisen equations of state were used to describe the condensed components, and the fluid detonation products were assumed to be polytropic for convenience. Because heat conduction was not treated explicitly in constructing these constitutive relationships, assumptions were required for their closure. Assumptions were made, (1) that no appreciable amount of heat is transferred into the interior of explosive and Al grains, and (2) that the heat transfer process between the Al_2O_3 covering the Al grains and the detonation products is efficient. As a result of the first assumption, burning explosive and reacting Al grains in an expansive flow behind the shock are constrained to their own isentropes and can adequately be described by their respective energy, pressure, volume equations of state. As a result of the second assumption, the Al_2O_3 and detonation products attain thermal equilibrium and the temperature equations of state of these components are required to formulate this condition.

Equations of state for the components in our reacting AP/Al composition were constructed to make our constitutive equation for this system practical. Our equation of state for Al was based on the Morse potential, and with values of the latent heat of vaporization, the specific heat at constant volume, and the Gruneisen parameter for Al from the literature, predicts shock wave states that are in excellent agreement with those determined experimentally up to 400 kbar. No equation of state was constructed for liquid Al, however, because melting of

condensed components was excluded from our first-generation model.

The equation of state for AP was based on shock wave and velocity of sound data and the assumption that its specific heat at constant volume and its Gruneisen parameter are constants. The unexpected high values for shock temperature calculated in the 300-400 kbar region, however, suggests that the validity of these assumptions must be considered in any future work on AP/Al compositions.

The first generation EOS, constructed for α-Al_2O_3 and amorphous γ-Al_2O_3, were based on shock-wave data for corundum and the assumptions that these oxides behave as linear elastic materials with constant specific heats at constant volume and constant Gruneisen parameters in the pressure range of interest. Literature values of the density, the standard heat of formation and standard entropy for α-Al_2O_3, and of the densities and standard heats of formation of amorphous γ-Al_2O_3 were used to evaluate Gibbs free energies at different pressures, and thereby obtain an estimate of the standard entropy of amorphous γ-Al_2O_3 and formulate a criterion for the formation of either α-Al_2O_3 or amorphous γ-Al_2O_3 in our reacting AP/Al mixture. It is important to note here that this description of Al_2O_3 is preliminary and needs to be improved in any future work that includes melting.

Our construction of a temperature equation of state for the polytropic fluid component was based on a complete equation of state, which provides the specific energy relationship already used for the detonation products, the thermodynamic identities for temperature and pressure, and the assumption that the specific heat at constant volume is constant. Here again the description of the fluid component must be improved in any future work on AP/Al and CHNO/Al compositions.

Certain aspects of steady-state detonation were considered to provide a better understanding of the dependence of the nonideal detonation process on reaction rates. Equations for estimating upper and lower limits for a steady-state reaction zone length were derived; shock wave data and the results of a TIGER code calculation for AP were used to obtain equations for the upper and lower limits of its reaction zone length in terms of its reaction zone time. Our prototype model for steady-state nonideal detonation was obtained by subjecting our previous treatment of the CHNO/Al composition to simplifying assumptions about the condensed components. The equations, derived for Chapman-Jouguet parameters in terms of the reaction coordinate describing the reaction of Al with detonation products, demonstrate clearly the dependence of steady-state nonideal detonation on this reaction and the reason for developing a realistic expression for its rate.

In the portion of our theoretical work presented in Section 3, we formulated rate expressions for the oxidation of Al and the decomposition of AP, which are needed to model nonideal detonation in our AP/Al compositions.

For the derivation of the rate equations for the Al reaction , the $Al/Al_2O_3/O_2$ system is treacted as a galvanic cell in which Al ions at the Al/Al_2O_3 interface are injected into the Al_2O_3 electrolyte and migrate toward the Al_2O_3/O_2 interface where Al_2O_3 is created.

In the construction of the rate model, it is assume that at the high pressures and

temperatures attained during the detonating process, β-Al_2O_3-like materials are present, which are known to exhibit anomalously high ionic conductivity because of the formation of tunnels through which ions can more easily pass. The equations describing the reaction process are presented and the rate constant, ionic conductivity, and mobility are calculated. This results in a rate constant that is an Arrhenius term multiplied by a factor proportional to $T^{7/32}p^{3/16}$.

It is concluded that

a. Al_2O_3 forms primarily at the Al_2O_3/O_2 interface. This is based on the excessive time it would take for the heat of reaction to diffuse from the Al/Al_2O_3 interface into the fluid products of the AP reaction.

b. Tunnels as ion conduits (or some similar scheme) are necessary in order to account for the high conductivity required to produce the observed reaction rates.

The reaction rate of AP is thought to be dominated by thermal relaxation processes, the volume and temperature dependences of which are estimated. The time it takes for energy to transfer from the acoustic vibrations of the AP molecule into its vibronic modes is seen to be long compared to other processes. It is assumed that reaction begins with the excitation of vibronic modes and that the thermal relaxation time is governed by energy transfer from acoustic modes into the lowest frequency vibronic ("doorway") mode from which energy is fed much more quickly into other vibronic modes.

The time necessary to excite a critical vibronic mode therefore is inversely proportional to the rate at which energy enters the doorway mode. This rate is dependent on the ratio of the doorway frequency to the highest frequency of the acoustic modes and is a minimum if the ratio is one. The rate is also volume-dependent because of the change of the acoustic mode frequencies with volume.

The rate equations developed here for the production of both Al_2O_3 and the explosive products of AP are not especially specific to these substances. They should apply as well to a number of explosives, oxidizers, and metals when appropriate substitutions for the values of the key parameters are made.

4.2. Summary of Progress vs. Proposed Tasks

The work described in Sections 2 and 3 of this report followed in general along the lines described in the Phase I Scope of Work in our proposal of 14 July 1994, but deviated in some important ways.

Task 1 of the Scope of Work sought to "develop a preliminary model for transport and kinetics mechanism[s] that determine the energy conversion and energy release rates in a *totally nonideal* explosive, such as an AP/Al mixture, ..." Section 3 of this report describes a theoretical model of the kinetics of the AP, Al, and Al_2O_3 interactions, which is far more complex and sophisticated, albeit preliminary, than attempted previously. The heat conduction processes are handled implicity in both Sections 2 and 3.

Task 3 sought to "examine different equations of state models as candidates for representing the products of metal/fuel/oxidizer/CHNOF explosive mixtures and metal fuel/oxidizer mixtures ..." Inasmuch as only an AP/Al mixture was to be considered (by Task 1), the most important detonation products are N_2, O_2, H_2O, Cl_2, and α- and amorphous Al_2O_3 (solid). Section 3 contains the equations of state, both E,P,V and T,P,V, derived for Al_2O_3. Equations of state for Al and AP as well as polytropic equations of state for CHNO detonation products that react with Al are also derived.

Task 2 was to "insert the preliminary model of Task 1 into a hydrodynamic code and calculate the failure diameter of a charge..."; Task 4 was "use a 1-D hydrocode to calculate the underwater bubble expansion to the first maximum...using the results from Tasks 1 and 3 ..." Early on, we started work on Task 4 but quickly dropped it, as well as Task 2. We decided to dedicate almost the entire effort to the much more important problems of developing the physical models of the kinetics of the AP/Al reaction, the development of the needed temperature equations of state for reactants and products, particularly to accomodate our assumption that the Al_2O_3 and detonation products are in thermal equilibrium, and to describe a phenomenological model based on fundamental physical principles.

The insertion of the physical models developed in Phase I into hydrocodes has been deferred to Phase II because of time constraints.

4.3. Recommendations.

The thermo-hydrodynamic model presented in this report is based on fundamental physical principles and provides a firm foundation for a first-generation hydrocode for investigating the nonideal detonation process in explosives containing Al. In addition, it is more realistic than many currently used in hydrocodes because, (1) untenable assumptions, such as the attainment of thermal equilibrium in the reacting explosive mixture, have been removed, and (2) the need for empirical fits of the rate equations has been eliminated. Nevertheless, our thermo-hydrodynamic model is clearly limited by restrictive assumptions, imposed by Phase I time constraints.

Proposed tasks for a Phase II program, which follow naturally from the work performed in Phase I and are needed to remove the latter's restrictive assumptions, are listed below:

1. Incorporate the first-generation model into a hydrocode, and validate it by performing a series of 1-dimensional, hydrodynamic calculations for AP/Al mixtures and comparing their detonation velocities with experimental data.

2. Extend our treatment of AP/Al and CHNO/Al compositions by including porosity.

3. In parallel with other recommendations above and below, incorporate as modules into an existing 2-dimensional flow hydrocode, e.g., CALE, the first- and subsequent-generation models, perform calculations for AP/Al and AP/CHNO/Al mixtures, and compare their results with experimental data available from Moby-Dick experiments at NSWC and underwater detonation experiments, including the bubble oscillation phase.

4. Extend the reaction schemes developed for AP/Al and CHNO/Al compositions in Phase I, by including the reaction of Al with H_2O in the AP/Al system and the reaction of Al with CO_2 in the CHNO/Al system.

5. Examine the mechanism of heat transfer in reacting explosive mixtures containing Al, with particular emphasis on late time.

6. Remove the restrictive assumptions that the values of C_v and Γ are constants for unreacted explosives and then construct more realistic EOS for unreacted AP and a prototype CHNO explosive.

7. Improve the equations of state of α-Al_2O_3 and amorphous γ-Al_2O_3 and formulate, based on Gibbs free energy considerations, a more basic criterion for the conversion of one into the other.

8. Consider melting of Al and Al_2O_3 in the reacting AP/Al and CHNO/Al mixtures.

9. Replace the polytropic EOS for the fluid detonation products by a more fundamental EOS based on statistical mechanics of the type developed and implemented by F.H. Ree, W.B. Brown and H.D. Jones and F. Zerilli.

10. Extend our thermo-hydrodynamic modeling to reacting AP/CHNO explosive/Al mixtures.

11. Investigate the intermediate oxidation states of Al, e.g., Al_2O_2 and AlO_2, to ascertain if other Al oxides are formed in rate controlling steps in the formation of Al_2O_3.

12. Include secondary oxygen sources, such as H_2O, and CO_2, in the reaction rate expression for Al, and consider its oxidation by chlorine.

13. Examine the effect of replacing Al with another metal.

REFERENCES

1. W. Fickett and W. C. Davis, *Detonation* (University of California Press, Berkeley, CA, 1979), Chap. 2.
2. R. Courant and K. O. Friedrichs, S*upersonic Flow and Shock Waves*, (Interscience Publishers, Inc. New York, 1948), Chapter III.
3. C. L. Mader, *Numerical Modeling of Detonations*, (University of California Press, Berkeley, CA, 1979.) Chapter 2.
4. M. Cowperthwaite, Nonideal Detonation in Composite CHNO Explosives Containing Aluminum, SRI International Final Report, SRI Project 8570, Contract No. N60921-90-C-0068, February 28, 1991.
5. See, for example, the review by E. Anderson, "Explosives" in Progress in Astronautics and Aeronautics, Vol. 155, pp. 81-163. (AIAA Publications).
6. D. Price, et al, "Explosive Behavior of Aluminized Ammonium Perchlorate, NOLTR 72-15 (May 1972); see also Report N60921-D-0024/DO 0129, Advanced Technology and Research Corp., Laurel, MD.
7. D. Price, "Critical Parameters for Detonation Propagation and Initiation of Solid Explosives," NSWC TR 80-339 (9/10/81).
8. M.J. Kamlet and S.J. Jacobs, J. Chem. Phys. **48**, 23 (1968)
9. J.W. Enig, "Modeling of Role of Thermal Hot Spots in the Shock-to-Detonation Transition in Energetic Materials," Air Force Armament Technology Laboratory Report AFATL-TR-89-111 (30 Sep 1989); also Enig Associates, Inc. Report No. ENIG 89-2.
10. D.J. Pastine, J. Appl. Phys. **35**, 3407 (1964)
11. F.W. Sandstrom, P.A. Persson, and B. Olinger, High-Pressure Science and Technology - 1993, (AIP Press, AIP Conference Proceedings 309, Part 2, New York) p. 1409.
12. B.M. Dobratz and P.C. Crawford, *LLNL Explosives Handbook*, Lawrence Livermore National Laboratory Report UCRL-52997 Change 2 (1985), p. 19-7.
13. R.G. McQueen, S.P. Marsh, J.W. Taylor, J.N. Fritz, and W. J. Carter, "The Equation of State of Solids from Shock Wave Studies," in *High-Velocity Impact Phenomena*, ed. R. Kinslow (Academic Press, New York, NY, 1970)
14. J. W. Enig, "Methods for the Derivation of Equations of State, "Naval Ordnance Laboratory (now Naval Surface Warfare Center) Report TN 5454 (Feb 1962); for a description of same theory in more available publications, see M. Cowperthwaite, "Relationships Between Incomplete Equations of State," J. Franklin Inst. **287**, 379 (1969) and W. Fickett and W. C. Davis, *Detonation*, p. 121 (Univ. of California Press, Berkeley, CA, 1979).
15. *LASL Shock Hugoniot Data*, ed. S.P. Marsh (University of California Press, Berkeley, CA, 1980).
16. *Tables of Integral Transforms Vol. 1*, ed. A. Erdelyi, p. 308 (McGraw-Hill Book Co., Inc. NY, 1954).
17. *Higher Transcendental Functions Vol I*, ed. A. Erdelyi, pp. 56, 110 (McGraw-Hill Book Co., Inc., NY, 1954).
18. *Handbook of Chemistry and Physics*, ed. R.C. Weast, 66th Edition 1985-1986, CRC Press, 1985, p. B-69 and D-51.
19. A.J. Brock and M.J. Pryor, Corr. Sci. **12**, 199, 1973.
20. M. Cowperthwaite and W.H. Zwisler, Sixth Symposium (Int.) on Detonation, 162-173, ACR-221, ONR, Dept. of the Navy (1966).
21. Reference Ref. 21, pp 8-21 - 8-23.

22. J.D. Weeks, D. Chandler, and H.C. Anderson, J. Chem. Phys. **54**, 5237(1971).
23. F.H. Ree, J. Chem. Phys. **84**, 5845(1985).
24. W.B. Brown, J. Chem. Phys. **87**, 566(1987).
25. H.D. Jones and F.J. Zerilli, J. Appl. Phys. **69**, 3893(1991).
26. I. Prigogine and R. Defay, *Chemical Thermodynamics*, (Longmann Green and Co., London, 1954), Chapter IV.
27. C. Wagner, Z., J. Physik. Chem. **21B**, 25(1933); **32B**, 447(1936); **40B**, 455 (1938).
28. C. Wagner and K. Grunwald, Trans. Faraday Soc. **34** 851 (1938)
29. H.H. Uhlig, *The Corrosion Handbook*, (John Wiley & Sons, New York & London, 1948).
30. C. Wagner, Corr. Sci. **13**, 23 (1973).
31. U.R. Evans, *Corrosion and Oxidation of Metals*, Supplementaty Vol. 2 (Edward Arnold, London, 1976).
32. A.J. Brock and M.J. Pryor, Corr. Sci. **13**, 199 (1973).
33. W.E. Garner, *Chemistry of the Solid State*, (Butterworths, London, 1955).
34. L. Young, *Anodic Oxide Films*, (Academic Press, New York, 1961).
35. A.S. Nowick and J.J. Burton, *Diffusion in Solids*, (Academic Press, New York, 1975).
36. P. Hagen Miller and W. Van Gool, *Solid Electrolytes*,(Academic Press, New York, 1978).
37. G.W. Castellan, *Physical Chemistry*, pp 352-353 (Addison-Wesley, Reading, 1964).
38. P.J. Miller and R.H. Gurguis, Proc. Mat. Res. Soc. Symp. **296**, 299 (1993); P.J. Miller and R.H. Guirguis, Proc. of Joint AIRAPT/APS Meeting, 28 Jun-2 July 1993, Colorodo Springs, CO; R.H. Guirguis and P.J. Miller, Tenth Symposium (Int.) on Detonation, pp. 675-682, 12-16 Jul 1993, Boston, MA (to appear).
39. G. Bjarnholt and R. Holmberg, Sixth Symposium (Int.) on Detonation, 540-566, ACR-221, ONR, Dept. of the Navy (1966).
40. R.R. McGuire, *et al*, Seventh Symposium (Int.) on Detonation, 940-951, NSWC MP 82-334, Naval Surface Weapons Center, Dahlgran, VA.
41. S. Goldstein and J.N. Johnson, Seventh Symposium (Int.) on Detonation, 1016-1023, NSWC, MP 82-334, Naval Surface Weapons Center, Dahlgran, VA.
42. I.B Akst, Ninth Symposium (Int.) on Detonation, 478-488, OCNR 113291-7, Office of the Chief of Naval Research, Arlington, VA.
43. E. O'Connor, "Shock Induced Reaction Mechanisms of Metal-Loaded Explosives," Masters Thesis, New Mexico Institute of Mining and Technology, Socorro, N.M.
44. J.E. Mayer and M.G. Mayer, *Statistical Mechanics*, (John Wiley and Sons, New York, 1961).
45. C. Kittel, *Solid State Physics*, pp 477-479 (John Wiley and Sons, London, 1957).
46. D.J. Pastine, H.D. Jones, *et al*, *High Pressure Science and Technology*, **2**, 364 (Plenum Publishing Corp., New York, 1979).
47. D.J. Pastine, Phys. Rev. **175**, 905 (1968).
48. D.J. Pastine, Phys. Rev. Lett. **23**, 1508 (1969).
49. See, for example, DD. Dlott and M.D. Fayer, J. Chem. Phys. **92**, 3798 (1990).

APPENDIX A. A MODEL FOR STEADY-STATE REACTION ZONE (SSRZ) TIMES

Our treatment of steady-state (SS) detonation here is based on the hypothesis that the global decomposition of a conventional condensed explosive is pressure dependent. In this case, it is significant to consider how SSRZ times are governed by an explosive's pressure-dependent burning rate because the classical treatment of the dependence of the SSRZ on particle size is based on the assumption that the explosive burns at a constant rate. Accordingly, we develop a prototype model for a SSRZ in order to investigate the relationship between an explosive's SSRZ time and its burning rate. To provide the necessary background for this development, we first present the conservation equations and Chapman-Jouguet (CJ) conditions for a SS detonation wave.

Equations for a SSRZ

We use the subscripts x and p to denote the explosive and its products, the subscript H to denote the shocked state, and either a superscript or a subscript 0 to denote the standard state of the explosive and the detonation products, i.e., at pressure p_0 and temperatures T_0. Recalling that the Rankine-Hugoniot (RH) jump conditions are first integrals of the differential equations expressing the conservation laws when the flow has attained a SS, we write the equation governing our SSRZ as

$$\rho(D-u)=\rho_0 D, \tag{A.1}$$

$$p=\rho_0 D^2(1-v/v_0), \tag{A.2}$$

$$e-e_x^0=pv_0(1-v/v_0)/2, \tag{A.3}$$

with D and u used, respectively, to denote the detonation velocity and the particle velocity, and $p_0=0$. Equation (A.1) expresses the conservation of mass, Eq. (A.2) expresses the conservation of mass and momentum, Eq. (A.3) expresses the conservation of mass, momentum, and energy, and the equations governing the shock at the front of the SSRZ are obtained by putting a subscript H on the variables ρ,u,p,v and e in Equations (A.1), (A.2), and (A.3).

To continue this treatment of our SSRZ, we introduce the sound speed c, define the adiabatic index k by the equation, $c^2=kpv$, and recall that the SSRZ terminates at the CJ state where the flows become sonic. Using the subscript j to denote the CJ state, this sonic condition is expressed by the equations

$$D-u_j=c_j. \tag{A.4}$$

The combination of the equations $\rho_j c_j=\rho_0 D$, $c_j^2=k_j p_j v_j$, and Eq. (A.2) written for the CJ state then gives the well known equations for v,u,c, and ρ in the CJ state as

$$v_j/v_0=k_j/(k_j+1), \tag{A.5}$$

$$k_j u_j=c_j=Dk_j/(k_j+1), \tag{A.6}$$

$$p_j=\rho_0 D^2/(k_j+1). \tag{A.7}$$

We finally note that the relationship between D and the specific chemical energy q liberated by a particle passing through the SSRZ is derived by combining the $e=e(p,v)$ equation of state for the detonation products with the following equation:

$$e_j-e_x^0=D^2/2(k_j+1)^2 \tag{A.8}$$

obtained by combining Eqs. (A.5) and (A.7) with Eq. (A.3) written for the CJ state.

Calculations of SSRZ Times

For the sake of tractability, *we assumed that the shocked explosive is incompressible* with a volume $\bar{v}=v_H$ and a Gruneisen parameter $\Gamma=\bar{v}(\partial p/\partial e_x)$. In this case, with λ used to denote the mass fraction of decomposed explosive, we can write the mixture rules for the specific volume and specific energy of the explosive and its products as

$$v=(1-\lambda)\bar{v}+\lambda v_p \tag{A.9}$$

$$e=(1-\lambda)e_x+\lambda e_p \tag{A.10}$$

With the added assumption that $p_x=p_p=p$, the $e_x=e_x(p,\bar{v})$ and $e_p=e_p(p,v_p)$ equations of state are then required to derive a constitutive equation for e in terms of p,v, and $\bar{v}$. We write the equation for e_x as

$$e_x - e_x^0 = \frac{p\bar{v}}{\Gamma} + \frac{p_H v_0}{2}\left[1-\left(1+\frac{2}{\Gamma}\right)\frac{v_H}{v_0}\right] . \tag{A.11}$$

We assume, again for tractability, that the explosive's products are polytropic with an index γ and write the equation for e_p as

$$e_p = e_p^0 + \frac{pv_p}{\gamma-1} . \tag{A.12}$$

The combination of Eqs. (A.9)-(A.12) allows us to write the constitutive equation for e for our decomposing explosive as

$$e = e_x^0 - \lambda q + \frac{pv}{\gamma-1} + (1-\lambda)v_0\left[\frac{p\bar{V}}{\gamma-1} + \frac{p_H}{2}\phi\right] \tag{A.13}$$

with the specific heat of decomposition $q=-(e_p^0-e_x^0)$, $\bar{V}=((\gamma-1)/\Gamma-1)\bar{v}/v_0$, and $\phi=1-(1+2/\Gamma)v_H/v_0$.

It is now convenient to derive the relationships between k and γ and D^2 and q. We first use the thermodynamic identity for the sound speed and $c^2=kpv$, which yield

$$k\frac{p}{v} = \frac{p + \dfrac{\partial e}{\partial v}}{\dfrac{\partial e}{\partial p}} , \tag{A.14}$$

and the equations for the partial derivatives of e derived from Eq. (A.13) to obtain the equation relating k and γ as,

$$k = \frac{\gamma v}{v+(1-\lambda)v_0\bar{V}} . \tag{A.15}$$

Setting $k=k_j$ and $v=v_j$ in Eq. (A.15) when $\lambda=1$, then shows that $k_j=\gamma$ at the end of the reaction zone. Combining the equations obtained by setting $k_j=\gamma$ in Eq. (A.8) and setting $\lambda=1$, $e=e_j$, $v=v_j=\gamma v_0/(\gamma+1)$, and $p_j=\rho_0 D^2/(\gamma+1)$ in Eq. (A.13) gives the well-known equation relating D and q:

$$D^2 = 2(\gamma^2-1)q . \tag{A.16}$$

The equations, relating λ and v and λ and p in the SSRZ, can now be derived from Eqs. (A.2), (A.3), (A.13) and (A.16) as follows. We substitute the expressions for p and q from Eqs. (A.2) and (A.16) into the equation obtained by eliminating e-e_x^0 between Eqs. (A.3) and (A.13) to derive, after some manipulation, the following equation relating λ and v in the SSRZ:

$$1-\lambda = \frac{[\gamma-(\gamma+1)\dfrac{v}{v_0}]^2}{1+2(\gamma+1)\bar{V}(1-\dfrac{v}{v_0})+(\gamma^2-1)\phi(1-\dfrac{v_H}{v_0})} . \tag{A.17}$$

The more interesting equation for our purpose here, that relates λ and p in the SSRZ, is obtained by combining Eqs. (A.17) and (A.2) as

$$1-\lambda = \frac{(p/p_j-1)^2}{1+2\bar{V}\dfrac{p}{p_j}+(\gamma-1)\phi\dfrac{p_H}{p_j}} = F(\frac{p}{p_j}, \frac{p_H}{p_j}) . \tag{A.18}$$

Because Eq. (A.18) will be used to calculate SSRZ times, it is convenient to consider a typical condensed explosive so that different values of Γ can be used to evaluate the parameters $\bar{V}$ and ϕ. We consider a typical explosive with the parameters: ρ_0=1.76 g/cc, D=7.4 mm/μsec, γ=3, p_j = 240.9 kbar, p_H=300 kbar and v_H/v_0=0.6887. The two cases, when $\bar{V}$=0 and ϕ=0, are of particular interest here. When $\bar{V}$=0 and $\Gamma=\gamma-1=2$, Eq. (A.18) becomes

$$1-\lambda = \frac{(\dfrac{p}{p_j}-1)^2}{1-a\dfrac{p_H}{p_j}} \tag{A.18.1}$$

with a=0.7548, and when, ϕ=0 and Γ=4.425, Eq. (A.18) becomes

$$1-\lambda = \frac{(\frac{p}{p_j}-1)^2}{(1-a\frac{p}{p_j})} . \qquad \text{(A.18.2)}$$

Before we can derive an equation for SSRZ times, we must specify an expression for the time rate of decomposition of the explosive, $d\lambda/dt$, in terms of the state variables, where t is the time. Here, we assume that our shocked, incompressible explosive grains are spherical, have an initial radius R_i, and burn with a pressure-dependent rate governed by the equation

$$\frac{dR}{dt} = -A_n p^n \qquad \text{(A.19)}$$

with n a variable parameter. In this case, the equation relating λ to the grain radius R is,

$$\lambda = 1-(\frac{R}{R_i})^3 , \qquad \text{(A.20)}$$

and the equation for the rate of decomposition follows by differentiating Eq. (A.20) as

$$\frac{d\lambda}{dt} = -\frac{3}{R_i}(\frac{R}{R_i})^2\frac{dR}{dt} . \qquad \text{(A.21)}$$

The combination of Eqs. (A.21), (A.20), and (A.19) then gives the equation for the rate of decomposition of our explosive in terms of λ and p as

$$\frac{d\lambda}{dt} = \frac{3}{R_i}(1-\lambda)^{\frac{2}{3}}A_n p^n . \qquad \text{(A.22)}$$

We now use Eq. (A.19) to define the characteristic time α_n as

$$\frac{1}{\alpha_n} = \frac{A_n p_H^n}{R_i} = -\frac{1}{R_i}(\frac{dR}{dt})_i \qquad \text{(A.23)}$$

and rewrite Eq. (A.22) as

$$\frac{d\lambda}{dt} = \frac{3(1-\lambda)^{\frac{2}{3}}}{\alpha_n}(\frac{p_j}{p_H})^n(\frac{p}{p_j})^n . \qquad \text{(A.24)}$$

Our general procedure for calculating SSRZ times is to integrate the expression for dt/dp in the SSRZ, obtained in terms of p from Eq. (A.18) and (A.23), from $p/p_j=p_H/p_j$ to $p/p_j=1$. Here, we will exemplify this procedure for the case when $V=0$. When $V=0$, we equate the expression for $d\lambda/dt$, derived by differentiating Eq. (A.18.1), and the expression for $d\lambda/dt$, derived by combining Eq. (A.18.1) and (A.23) to eliminate $(1-\lambda)^{2/3}$, to obtain the following equation for dp/dt in the SSRZ:

$$-\frac{2}{[1-a\frac{p_H}{p_j}]^{\frac{1}{3}}}\left(\frac{p_H}{P_j}\right)^n\frac{dp}{dt} = 3\frac{p_j}{\alpha_n}\left(\frac{p}{p_j}-1\right)^{\frac{1}{3}}\left(\frac{p}{p_j}\right)^n . \tag{A.25}$$

Formally integrating Eq. (A.25), with $P=p/p_j$ and $P_H=p_H/p_j$, gives the equation for the SSRZ time t_n as

$$\frac{t_n}{\alpha_n} = \frac{-2P_H^{\,n}}{3(1-aP_H)^{\frac{1}{3}}}\int_{P_H}^{1}\frac{dP}{P^n(P-1)^{\frac{1}{3}}} = \frac{-2P_H^{\,n}}{3(1-aP_H)^{\frac{1}{3}}}I_n , \tag{A.26}$$

where I_n is the integral in Eq. (A.26). Combining Eq. (A.23) and (A.26) gives the equation

$$A_n = -\frac{2R_i}{3(p_j)^n(1-aP_H)^{\frac{1}{3}}}\left(\frac{I_n}{t_n}\right) , \tag{A.27}$$

which allows us to calculate A_n when R_i and n are known and the SSRZ parameters p_H, p_j, and t_n are also known.

We now set n=1 and evaluate I_1 to determine the relationship between t_1 and α_1. To reduce I_1 to a more recognizable form, we change the variable from P to y by setting $y^m=P-1$, and then set m=3 to obtain the equation

$$I_1 = 3\int_{y_H}^{0}\frac{y\,dy}{y^3+1} , \tag{A.28}$$

where $y_H=(P_H-1)^{1/3}=0.6258$. We now use

$$\int\frac{y\,dy}{1+y^3} = -\frac{1}{6}\ln\frac{(1+y)^2}{1-y+y^2}+\frac{1}{\sqrt{3}}\tan^{-1}\left(\frac{2y-1}{\sqrt{3}}\right) \tag{A.29}$$

to evaluate this integral between y_H=0.6258 and y=0, and find the following equation relating t_1 and α_1: $t_1=1.137\alpha_1$.

We now set n=2 and evaluate the integral

$$I_2 = \int_{P_H}^{1}\frac{dP}{P^2(P-1)^{\frac{1}{3}}} \tag{A.30}$$

to determine the relationship between t_2 and α_2. An operation using integration by parts, separation by partial fractions, and the change of variable $y^3=P-1$ allows us to write an equation for I_2 as

$$I_2 = -\frac{(P_H-1)^{\frac{2}{3}}}{P_H}+\frac{I_1}{3} . \tag{A.31}$$

Equations (A.26) and (A.31) then give the following equation relating t_2 and α_2: $t_2=1.30\alpha_2$.

It is clear that the results of these calculations are limited by our simple description of the explosive and its products. Nevertheless, they are significant for an explosive with a pressure dependent, decomposition rate because they show that the parameter A_n in its rate law can, in principle, be determined when n, the initial grain size, the ZND spike pressure, and the SSRZ time are known.

SECURITY CLASSIFICATION OF THIS PAGE

REPORT DOCUMENTATION PAGE

1a. REPORT SECURITY CLASSIFICATION: Unclassified	1b. RESTRICTIVE MARKINGS: None
2a. SECURITY CLASSIFICATION AUTHORITY	3. DISTRIBUTION/AVAILABILITY OF REPORT: Unlimited distribution
2b. DECLASSIFICATION/DOWNGRADING SCHEDULE	
4. PERFORMING ORGANIZATION REPORT NUMBER(S): ENIG TR 95-1	5. MONITORING ORGANIZATION REPORT NUMBER(S)
6a. NAME OF PERFORMING ORGANIZATION: Enig Associates, Inc. / 6b. OFFICE SYMBOL (If applicable)	7a. NAME OF MONITORING ORGANIZATION: Office of Naval Research
6c. ADDRESS (City, State, and ZIP Code): 11120 New Hampshire Ave., Suite 500 Silver Spring, MD 20904-2633	7b. ADDRESS (City, State, and ZIP Code): 800 N. Quincy Street Attn: Dr. Judah Goldwasser Arlington, VA 22217-5660
8a. NAME OF FUNDING/SPONSORING ORGANIZATION: Office of Naval Research / 8b. OFFICE SYMBOL (If applicable): Code 331	9. PROCUREMENT INSTRUMENT IDENTIFICATION NUMBER: Contract No. N00014-95-C-0154
8c. ADDRESS (City, State, and ZIP Code): 800 N. Quincy Street Attn: Dr. Judah Goldwasser Arlington, VA 22217-5660	10. SOURCE OF FUNDING NOS. — PROGRAM ELEMENT NO.: 333ww95sbir1 / PROJECT NO. / TASK NO. / WORK UNIT NO.

11. TITLE (Include Security Classification): Energetics of Late Chemical Reactions in Nonideal Underwater Detonations: Phase I, Preliminary Model Development

12. PERSONAL AUTHOR(S): Michael Cowperthwaite, D. John Pastine, Julius W. Enig

13a. TYPE OF REPORT	13b. TIME COVERED	14. DATE OF REPORT (Yr., Mo., Day)	15. PAGE COUNT
Final	FROM 950401 TO 950930	951010	73

16. SUPPLEMENTARY NOTATION

17. COSATI CODES			18. SUBJECT TERMS (Continue on reverse if necessary and identify by block number)
FIELD	GROUP	SUB. GR.	Underwater explosives, nonideal explosives, detonations, aluminized explosives, modeling, kinetics, equations of state, aluminum oxide

19. ABSTRACT

This report describes a preliminary model of kinetic and thermo-hydrodynamic processes that define the nonideal detonation of a *totally nonideal* explosive: an AP/Al mixture. Section 2 presents a thermo-hydrodynamic description of reactive explosive compositions containing aluminum and, in particular, a description of the nonideal detonation process in ammonium perchlorate/aluminum and CHNO explosive/Al compositions. The specific energy relationships for these reacting compositions were formulated with each component governed by its own equations of state. Mie-Gruneisen equations of state are derived, including the temperature, and used for the solid components, but the detonation products are treated as a polytropic fluid. Equations of state for steady-state detonation in AP and the prototype model for nonideal detonation in CHNO/Al composition are also presented. In Section 3 we present a theory describing the kinetic processes by which Al/Al_2O_3/AP products react. Key here is the application of the phenomenon of anomalously high ionic conduction, which are exhibited by the β-aluminas, through "tunnels" through which cations can move freely. This provides a plausible explanation of events in Al/explosive reactions. Statistical mechanical concepts are employed to provide reaction rate equations for Al and AP. The theoretical results of Sections 2 and 3 provides a preliminary physical model based on first principles, which will be integrated into a compressible flow code in the next phase of this work, which is to improve, extend, and validate the model.

20. DISTRIBUTION/AVAILABILITY OF ABSTRACT	21. ABSTRACT SECURITY CLASSIFICATION	
X UNCLASSIFIED/UNLIMITED ___ SAME AS RPT ___ DTIC USERS	Unclassified	
22a. NAME OF RESPONSIBLE INDIVIDUAL: Judah M. Goldwasser	22b. TELEPHONE NUMBER (Include Area Code): (703) 696-2164	22c. OFFICE SYMBOL: Code 331

DD FORM 1473, 84 MAR — 83 APR edition may be used until exhausted. All other editions are obsolete

SECURITY CLASSIFICATION OF THIS PAGE